Characterising the relative importance of photosynthetic and chemosynthetic primary production to consumers in a dystrophic lake

Kanishk P. Walavalkar

Student registration number: 3008817w

Course: MRes, Ecology and Environmental Biology

Project supervisor: Chris Harrod

Word count: 8406

Abstract (240/250 words)

The food web dynamics of dystrophic lakes remain poorly understood. To address this gap, we investigated the food web of Dubh Lochan, a small (0.07 km^2) dystrophic lake in western Scotland. Using carbon and nitrogen stable isotope analyses and diet and population assessments of perch *Perca fluviatilis*, we characterised trophic structure, basal energy sources, and the role of methane-derived carbon. Putative sources of primary producers were diverse (n = 10), but the phytoplankton community was very restricted. Consumer taxa included zooplankton, macroinvertebrates, and fish, spanning wide mean isotopic ranges ($\delta^{13}C$: –60‰ in methane-oxidising bacteria to –24.8‰ in reed beetle; $\delta^{15}N$: –4.9‰ in terrestrial leaf litter to 10.2‰ in pike). These gradients indicated multiple trophic transfers and clear evidence of energy flow. Mixing model outputs highlighted terrestrial leaf litter (mean% $\pm$ SD contributions: 19.2 % $\pm$ 8.5) as the dominant energy source for most consumers, although contributions varied among taxa. Littoral *Asellus aquaticus* ($\sim$ 21 %) showed strong reliance on ^{13}C-depleted methane-derived carbon, exceeding that of profundal chironomids ($\sim$15 %). Despite the presence of methane in the water column and isotopically distinct methane-derived carbon, photosynthetically-derived production remained the principal support of the food web. Perch, the numerically dominant fish, exhibited unusual ontogenetic dietary shifts with juveniles displaying high levels of cannibalism, while larger adults increasingly consumed chaoborid larvae. Our study resolves the relative contributions of photosynthetic and chemosynthetic pathways in a DOC-rich system, advancing understanding of trophic organisation in dystrophic lakes.

Introduction (749/1000-1500)

Inland waters, cover less than 1% of the Earth's surface, but play a disproportionate role in global carbon cycling (Downing *et al.* 2006; Cole *et al.* 2007; Liu *et al.* 2024). Lakes process carbon from both autochthonous (in-lake) and allochthonous (terrestrial) sources, transforming it into biomass, sediments, or greenhouse gases (Guillemette *et al.* 2017; Tranvik, Cole & Prairie 2018). These systems support primary production through two main pathways: photosynthesis, which uses light to fix inorganic carbon, and chemosynthesis, which relies on chemical energy from reduced compounds (Savvichev *et al.* 2020; Di Nezio *et al.* 2021) for carbon fixation. The balance between these pathways can vary widely depending on lake morphology, hydrology, land use, nutrient availability, light penetration, and organic matter inputs (Seekell *et al.* 2015; Olson, Solomon & Jones 2020). Understanding their relative importance is essential for informed resource management of systems that provide a diverse array of essential ecosystem services to society (Assessment 2005; Carpenter, Stanley & Vander Zanden 2011). Furthermore, this information is required to predict ecosystem responses to ongoing environmental change and assessing whether lakes act as net carbon sinks or sources (Bogard & del Giorgio 2016; Hessen *et al.* 2024).

Dystrophic lakes are nutrient-poor, acidic water bodies rich in terrestrial-derived dissolved organic carbon (tDOC), and are often associated with peatlands and boreal catchments (Milferstedt, Youngblut & Whitaker 2010; Jentzsch *et al.* 2024; Sabrekov *et al.* 2024). Their dark brown colour, caused by dissolved humic substances, limits light penetration and suppresses algal production (Kullberg *et al.* 1993; Karlsson *et al.* 2009) weakening traditional "green" photosynthesis-driven food webs (Newton *et al.* 2006). Instead, these lakes are typically supported by "brown" food webs, where energy is

derived from the respiration of detrital material by microbial consumers (Amblard *et al.* 1995; Tadonléké, Planas & Lucotte 2005). Microbial production in such systems can include heterotrophic bacteria utilising dissolved organic carbon (DOC) (Bergström & Jansson 2000; Tranvik *et al.* 2009) and fungi (Gessner & Chauvet 1994; Grossart *et al.* 2019). Methanotrophic bacteria (MOB) using methane as an energy source supporting chemosynthetic primary production (Kankaala *et al.* 2006; Jones & Grey 2011). Determining the relative importance of these pathways is key to understanding the structure, resilience and informed management of dystrophic lakes.

The role of methane-derived carbon in the functioning of lake ecosystems is of considerable current interest (Schorn *et al.* 2024). Methane (CH_4) is a potent greenhouse gas with a global warming potential over 80 times greater than carbon dioxide (CO_2) over a 20-year period and about 28 times greater over a 100-year timeframe (Armour *et al.* 2021). While ~60% of global emissions are anthropogenic (from agriculture, fossil fuel use, and waste), natural sources, especially from inland waters, account for the remainder (Saunois *et al.* 2019; Xi *et al.* 2023). Despite their small surface area, freshwaters contribute substantially to natural methane fluxes, making them key players in both regional and global methane budgets (Bastviken *et al.* 2011; DelSontro, Beaulieu & Downing 2018).

In lakes, methane is produced via microbial methanogenesis in anoxic sediments and hypolimnic waters, and can be oxidised by methane-oxidising bacteria (MOB), converting it into CO_2 or biomass (Youngblut, Dell'aringa & Whitaker 2014; Yang *et al.* 2025). This methane can escape to the atmosphere via diffusion (diffusive flux), bubbling (ebullition flux), or plant-mediated transport (vegetative flux), or it can be oxidised by methane-oxidising bacteria (MOB) at oxic-anoxic interfaces (Schorn *et al.*

2024). This oxidation not only mitigates greenhouse gas emissions but can also generate microbial biomass that may enter food webs, forming a chemosynthetic pathway parallel to photosynthesis (Barber, Burke Jr & Sackett 1988). However, the extent to which methane-derived carbon supports aquatic consumers varies greatly among systems (Kritzberg *et al.* 2004; Lau *et al.* 2014b).

Stable isotope studies have shown that isotopically light (i.e. depleted in ^{13}C) methane-derived carbon can be traced from MOB to zooplankton, macroinvertebrates, and even fish (Ravinet *et al.* 2010; Sanseverino *et al.* 2012). Methane can contribute substantially to lake consumer biomass (Deines, Bodelier & Eller 2007; Tsuchiya *et al.* 2020) but in other systems, its role appears minor relative to algal or detrital sources. This variability highlights the need for site-specific studies that compare potential basal sources directly, rather than assuming a dominant role for any one pathway.

Understanding the integration of multiple basal sources into food webs requires robust tools. Traditional approaches such as stomach content analysis (SCA) (Egerton 2007), while valuable for identifying recent feeding activity to high taxonomic levels, can miss cryptic pathways such as methane-derived primary production or miss functional variation within prey taxa (Harrod & Grey 2006). In contrast, stable isotope analysis offers long-term integration of diet and energy source information (Fry 1991; Harrod & Stallings 2022). Carbon isotopes ($\delta^{13}C$) are especially useful in tracing carbon flow (Finlay & Kendall 2007; Schenk *et al.* 2021). Nitrogen isotopes ($\delta^{15}N$), which become enriched by ~3–4‰ with each trophic step, provide complementary information on an organism's trophic position (Post 2002). When combined, $\delta^{13}C$ and $\delta^{15}N$ values can be used to construct isotopic niches and infer both energy sources and food web structure (Fry 1991; Wada 2009; Eglite, Mohm & Dierking 2023).

However, interpretation of isotopic data must be undertaken with care. Issues such as variable baseline $\delta^{13}C$ values (Belle & Cabana 2020; Yun *et al.* 2024), overlapping source values (Phillips & Gregg 2001), and physiological variation in isotope assimilation can complicate the resolution of food web pathways (Aberle & Malzahn 2007; Yeakel *et al.* 2016a). These challenges are particularly pronounced in DOC-rich, nutrient-poor lakes, where microbial and detrital food webs dominate and where clear-cut source discrimination is difficult (de Kluijver *et al.* 2014; Lammers, Reichart & Middelburg 2017). Nevertheless, the increasing use of Bayesian mixing models (Phillips *et al.* 2014), compound-specific isotope analysis (CSIA) (Burian *et al.* 2020), and other high-resolution techniques is allowing researchers to disentangle these complex trophic interactions with growing confidence (Galloway *et al.* 2015).

Here, we investigate the food web of Dubh Lochan (56.132°N, 4.614°W), a small (<0.1 km^2) dystrophic lake in western Scotland. This system's high DOC, acidic conditions (Shafi 1969), and low nutrient availability (Tippett 1994) suggest a potential reliance on microbial pathways, including heterotrophic and possibly chemosynthetic production. We aimed to (1) characterise consumer community composition, (2) using stable isotope analysis (SIA: $\delta^{13}C$ and $\delta^{15}N$) alongside stomach content analysis (SCA), characterise trophic structure including the relative importance of different putative energetic pathways to consumers, (3) including the extent to which methane-derived carbon contributes to the food web. Finally, (4), we focus on the trophic ecology of the perch *Perca fluviatilis*, examining population and intra-population variation in diet through SIA and SCA.

Materials and methods (2396/1000-1500)

Field based methods

Limnological sampling was conducted to quantify seasonal variation in key abiotic parameters, including dissolved oxygen, light penetration, and thermal stratification. A brief study on the diffusive flux of methane and carbon dioxide was conducted to confirm our assumptions about the lake's physical condition. These measurements were used to delineate distinct aquatic zones (e.g. epilimnion, metalimnion, hypolimnion), thereby providing the environmental context necessary for interpreting trophic interactions.

Subsequent biological sampling focused on assessing community composition, abundance, and spatial distribution. Organisms were also collected for further laboratory analyses (e.g. SIA, SCA), facilitating a comprehensive understanding of food web structure and energy flow.

Limnological sampling

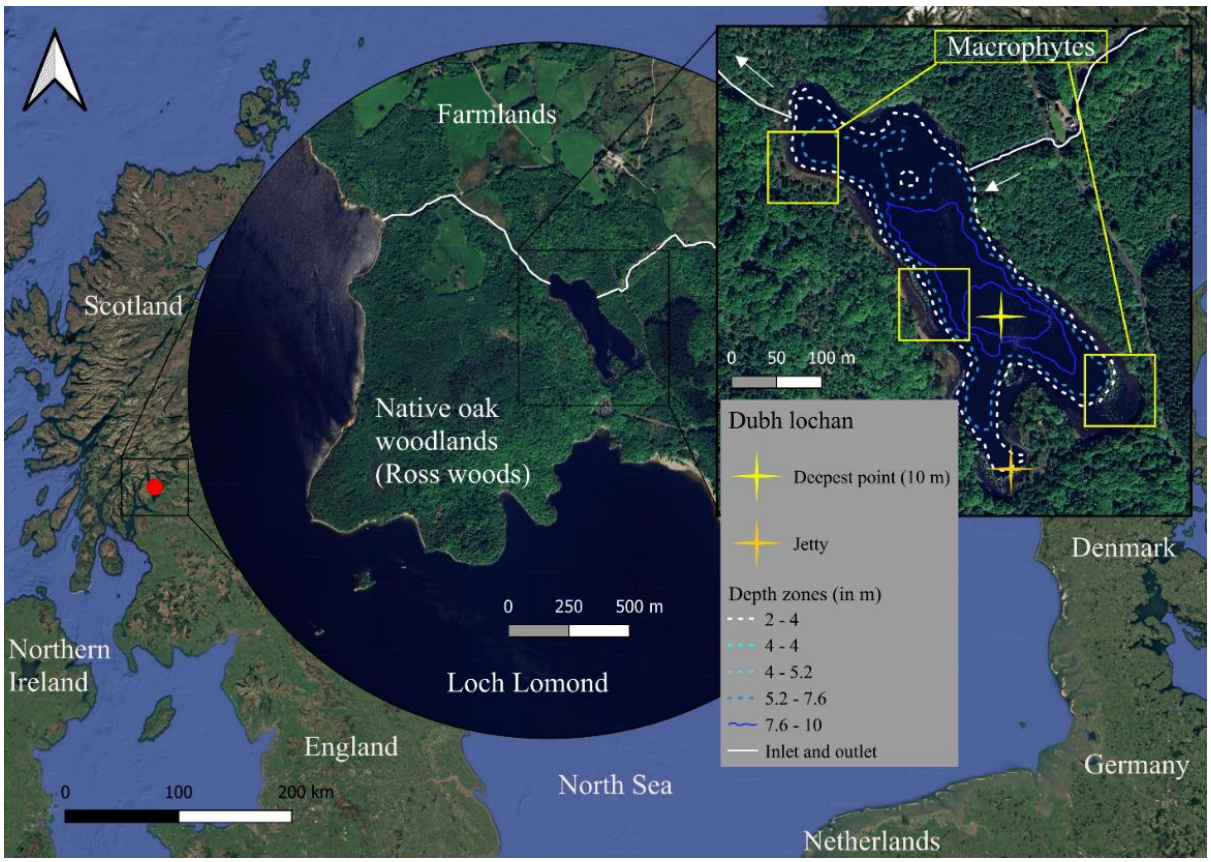

***Figure 1**. Study site and bathymetric data informing our pilot study*

Between 28 September 2024 and 24 July 2025, regular limnological surveys were conducted to assess vertical profiles of dissolved oxygen, temperature, and light availability within the Dubh Lochan (Fig. 1). Measurements were taken at the lake's deepest point (maximum depth: 10 m) from a small (3m) boat at weekly to biweekly intervals, limited to ice-free periods. All measurements were standardised by conducting sampling around local solar noon (approximately 12:00 p.m.) to minimise diel variation. Profiles were recorded at 0.5-meter depth intervals, with the surface designated as 0 meters. Light intensity was expressed as a percentage of incident surface irradiance to facilitate comparisons across depths and seasons.

In addition to thermal and oxygen profiling, a one-off assessment of dissolved methane (CH_4) and carbon dioxide (CO_2) concentration and stable isotope values ($\delta^{13}C$) was conducted via headspace equilibrium test (Magen *et al.* 2014) on 2 July 2025 in collaboration with Dr. Adrian Bass of the School of Geographical & Earth Sciences, University of Glasgow. Triplicate water samples were collected from four representative locations: (i) central deepest point (10m), (ii) south-eastern basin (6m depth), (iii) north-eastern riverine inlet, and (iv) northern outlet. At each location, samples were obtained from three discrete depths: surface, midwater, and bottom to capture vertical variation in greenhouse gas distribution.

A high-resolution bathymetric survey was also constructed using a Lowrance HD9 echo sounder, which simultaneously recorded spatial coordinates (x, y) and depth (z) as the boat navigated along pre-defined grid transects. The resulting dataset was processed in QGIS to generate a detailed bathymetric map, enabling spatial analysis of depth-related ecological patterns for targeted sampling.

Biological sampling

Primary producers were sampled to characterise the basal resources supporting the lake's food web, including northern, southern, western, and eastern shores, ensuring spatial coverage and representation of dominant species. Epiphytic biofilm was obtained by deploying and subsequently retrieving artificial substrates (like buoys and colonisation traps) that allowed for natural colonisation. Biofilm samples were scraped and collected for analysis.

Seston was sampled using horizontal surface tows with a phytoplankton net (30 cm mouth diameter, 66.5 cone, 20 μm mesh) to target suspended particulate autotrophs. Tows were performed in the pelagic zone at a consistent depth just below the surface,

ensuring standardised effort across sampling events. Particulate organic matter (POM) was sampled from the pelagic zone by collecting 30 L of lake water at a depth of 1 m using a 2.5 L deep water sampler. All samples were collected manually using clean, pre-rinsed equipment to avoid contamination and were immediately stored in appropriate containers for further processing and analysis. Replicate water samples were filtered on to 0.7 µm pre-combusted (550°C for 4 hours) 47 mm diameter glass fibre filters for subsequent stable isotope analysis.

Invertebrate sampling was conducted on 28 June, 30 June, and 15 July 2025. Benthic macroinvertebrates were collected using an Ekman grab at four depth strata (2, 6, 8 and 10 m). Retrieved sediments were sieved and organisms were sorted manually. Littoral invertebrates were sampled via standardised pond-net sweeps through submerged macrophytes and kick-sampling along the shallow shoreline.

Zooplankton sampling was carried out between 21 May and 12 June 2025 using vertical zooplankton net hauls (30 cm mouth diameter, 66.5 cm cone, 200 μm mesh) from the same depth zones used in benthic invertebrate sampling. To account for diel vertical migration patterns, sampling was conducted at three distinct times of day: early morning (02:00 – 05:00), midday (11:00 – 15:00), and night (22:00 – 00:00).

The fish community was sampled across multiple regions of the lake: north, south, east, west, northeast, northwest, southeast, southwest, and central, between 6 October 2024 and 4 July 2025. Sampling targeted a range of ecological zones, including the pelagic, littoral, and profundal habitats. A combination of gear types was employed to capture fish of varying sizes and functional groups: multi-panel benthic-set gill nets, floating gill nets and baited minnow traps. This multi-gear approach maximised coverage across depth gradients and habitat types. Sampling gear was deployed overnight and retrieved

within 24-hour intervals to minimise sampling-induced mortality and avoid excessive extraction of target and non-target organisms.

Sample processing

1. Macrophytes, Seston, and Biofilm: Leaf material from macrophytes, as well as seston and biofilm samples, were frozen (-20°C), oven-dried (60°C), and ground to a fine homogenous powder. Subsamples of 1.0-1.6 mg were used for SIA.
2. Particulate organic matter (POM): Nearly half of the GFF filter was used for each capsule. The filters were lightly scraped off the surface into the tin capsules. No pre-treatment was conducted.
3. Invertebrates: Whole-body specimens were collected, frozen, dried (60°C), and ground. The homogenous powder was weighed (0.2-0.6 mg) and analysed directly. For abundant taxa, three subsample triplicates were used for analysis.
4. Fish: Dorsal white muscle tissue was excised, frozen at -20°C, and subsequently oven-dried at 60°C. Dried tissue was weighed (0.2-0.6 mg) and encapsulated in tin for analysis.

Stomach content analysis

A total of 149 fish specimen were dissected for stomach content analysis from 6 October 2024 to 4 July 2025. These consisted of Eurasian perch (*Perca fluviatilis*, $n = 129$) and northern pike (*Esox lucius,* $n = 20$). Each fish was measured for fork length (± 1 mm) and blotted wet mass ($\pm$ 0.1 g) both before and after freezing at -20°C in individually labelled plastic bags.

Specimens were thawed at 4°C prior to dissection. Tissue samples were collected for multiple purposes: stomachs for dietary analysis, white muscle tissue for stable isotope

analysis, opercula for age estimation, and liver and ovary tissue for parallel undergraduate research projects. Each individual was sexed visually (classified as male, female, or immature) to account for possible sex-specific or ontogenetic variation in diet (Crim 1990).

Laboratory based methods

Limnological analyses

A total of 36 water samples were collected for the analysis of dissolved methane (CH_4), carbon dioxide (CO_2) and dissolved inorganic carbon (DIC) from 4 different sites at three distinct water depths (top, middle, bottom). All analyses were carried out in the School of Geographical and Earth Sciences of the University of Glasgow.

Following collection, the samples were transported to the laboratory, where headspace equilibration procedures were conducted. For each sample, 50 mL of lake water was withdrawn from a sealed 250 mL glass container and replaced with an equal volume of inert gas (nitrogen) in a closed-loop system to prevent atmospheric contamination. The sealed samples were equilibrated overnight at room temperature to allow for gas exchange between the liquid and headspace phases.

The equilibrated headspace gas was then analysed using a Cavity Ring-Down Spectrometer (CRDS: Picarro G2201-I, Santa Clara, CA, USA), which provides high precision measurements of the concentration and the carbon stable isotope values of CO_2 ($\delta^{13}CO_2$) and CH_4 ($\delta^{13}CH_4$). Two certified calibration standards were used to ensure analytical accuracy:

- Standard 1: $CH_4 = 1.8$ ppm, $CO_2 = 400$ ppm, $^{13}CH_4 = -47$ ‰, $^{13}CO_2 = -8.6$ ‰).
- Standard 2: $CH_4 = 10$ ppm, $CO_2 = 1000$ ppm, $^{13}CH_4 = -69$ ‰, $^{13}CO_2 = -20$ ‰)

Biological analyses

Primary producers, macroinvertebrates and zooplankton were subsequently sorted and identified in the laboratory using relevant keys and identification guides (Croft 1986; Greenhalgh & Ovenden 2007). This section outlines the laboratory procedures employed, with methods organised according to the type of analysis conducted.

Stable isotope analysis

A total of 251 biological samples collected between 6 October 2024 and 18 July 2025, a total of 251 biological samples were subsampled for stable isotope analysis, fish ($n = 137$), macrophytes and seston ($n = 35$), particulate organic matter ($n = 5$) and aquatic invertebrates ($n = 74$). All samples were analysed for carbon ($\delta^{13}C$) and nitrogen ($\delta^{15}N$) isotope composition using a Thermo Scientific™ IsoLink™ Flash Elemental Analyser coupled to a Delta V Advantage Isotope Ratio Mass Spectrometer (IRMS: Thermo Scientific, Bremen, Germany) working in continuous flow mode at the Stable Isotope Biogeochemistry Laboratory of the Department of Earth Sciences/Archaeology at Durham University.

Carbon isotope ratios were reported in standard delta notation (δ, per mil ‰) relative to Vienna Pee Dee Belemnite (VPDB). Nitrogen isotope ratios were expressed relative to atmospheric nitrogen (AIR).

Quality control and calibration

Analytical accuracy and precision were maintained through routine inclusion of in-house reference materials, stringently calibrated against international standards,

Analytical precision ($\pm$ 2 S.D.) was typically ± 0.1‰ for $\delta^{13}C$ and <0.2‰ for $\delta^{15}N$ based on replicate standard and sample analyses.

Stomach content analysis

Stomach contents were extracted into petri dishes and identified to the lowest possible taxonomic level (typically to family) using a stereomicroscope and an identification key (Croft 1986). Each stomach was assessed for both fullness and digestion stage using the Alaska Fisheries Science Centre (AFSC 2015) scoring system:

- Fullness: 1 (empty) to 7 (distended)
- Digestion: 1 (empty) to 6 (no digestion evident)

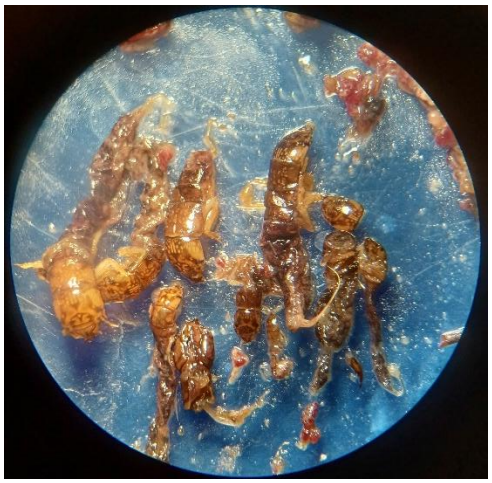

Figure 2. *Sialidae spp. larvae found in the stomach of perch caught in June 2025.*

A numerical estimate of prey abundance was made by counting unique, identifiable body parts (e.g. head capsules, carapaces, opercula). To complement and standardise this count, the points method (Hynes 1950; Manko 2016) was employed. This semi-quantitative method reduces observer bias and facilitates rapid assessment. Stomachs were visually assigned a total score of 20 (full), or 20-30 in the case of distended guts. Each prey item was then given a point value (1, 2, 4, 8 or 16) based on its relative volume or contribution to the stomach contents, following established protocols.

Ageing

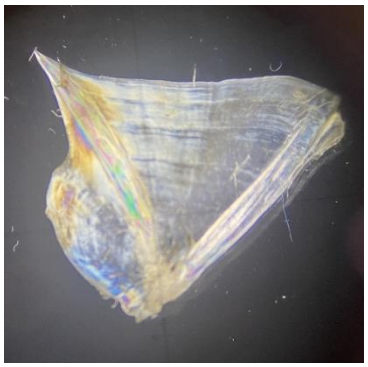

Figure 3. *Perch operculum under iridescent light showing the growth annuli*

Opercula were collected from the dominant member of the Dubh Lochan fish community *Perca fluviatilis* (European perch) for age estimation. Opercular length was measured as the approximate perpendicular from the focus to the posterior edge using a digital Vernier calliper ($\pm$0.01 mm accuracy) (Coyne, Connor & Kelly 2019). Maturity classes were assigned visually based on annuli counts (Le Cren 1947), following the protocol outlined by Coyne, Connor and Kelly (2019) using '+' convention (Le Cren 1947). Individuals were assigned to three maturity classes: young-of-the-year (YOY; age 0), juveniles (ages 1-3), and adults (ages $\geq$ 3).

Statistical methods

Population structure

The population structure of the dominant fish species was examined to characterise key consumer dynamics. For European perch *(Perca fluviatilis)*, sex-specific differences in demographic and morphological traits were assessed. Analyses included sex ratio, mass-length differences, the allometric length-weight relationship, and condition. Age structure by sex was also visualised (Appendix A4), along with size-at-age by sex

(Appendix A5), to assess growth trajectories, recruitment patterns, and potential cohort structures. The length at 50% maturity was also calculated following Ogle (2018).

Sex ratio deviations from parity were tested using a chi-squared goodness-of-fit test. Differences in length and mass between sexes were assessed using both parametric (Welch's two-sample *t*-test) and non-parametric (Wilcoxon rank-sum test) approaches to account for potential violations of normality assumptions. The mass-length relationship was modelled to determine growth type (isometric vs. allometric), and an ANCOVA was applied to test whether this relationship differed between sexes.

Diet characterisation

The points volumetric method was used to calculate the percent contribution of each prey item to the diet of the corresponding fish.

$$\%P_i = \frac{P_i}{P_t} \times 100$$

Where $\%P_i$ is the percent contribution of item i, P_i is the value of points allotted to the item i, and P_t is the number of points allotted to the stomach (Manko 2016).

The frequency of occurrence (FO) was also calculated using the presence-absence approach as it provides a useful indication of the relative importance of different prey resources and allows direct comparison with other studies, e.g. Shafi (1969).

A permutational multivariate analysis of variance (PERMANOVA) based on a Bray-Curtis dissimilarity matrix of square root transformed prey count data was used to inspect the variance in diet by groups of size, age and sex using *adonis2* routine in the R package vegan (Oksanen *et al.* 2001). The quantile method was used to accurately compartmentalise the perch into 'small (46 to 66 mm)', 'medium (70 to 126 mm)' and

'large (128 to 271 mm)' size classes. A subsequent SIMPER analysis was used to examine which prey taxa were driving the major differences between the different size classes.

Stable isotope analysis

Stable isotope data from fish white muscle tissue was first corrected for lipids using Kiljunen *et al.* (2006). Stable isotope data were plotted to provide $\delta^{15}N$-$\delta^{13}C$ biplots to characterise the Dubh Lochan food web. This was followed by a visualisation of an ordered boxplot of all taxa that were sampled from the Lochan (Appendices A9, A10). Stable isotope values for MOB were not measured from Dubh Lochan during this and values were estimated using mean ($\pm$ SD values) from the literature (Lau *et al.* 2014a), following DelVecchia, Stanford and Xu (2016).

Mixing models

In order to transform stable isotope data into estimates of the relative contribution of different resources to consumers, we used Bayesian Stable Isotope Mixing Models (Phillips 2012). The R package *simmr* (Parnell & Parnell 2019) was used to run mixing models that examined the relative contributions of 1) different primary producers to invertebrate and fish consumers and 2) the relative contribution of different putative prey to fish consumers. For the first set of mixing models, we used the general ecosystem level trophic factors (TDFs: mean $\pm$ SD: $\Delta^{13}C = 0.4 \pm 1.3‰$, $\Delta^{15}N = 3.4 \pm 1$ provided by Post (2002). TDFs were adjusted for the putative trophic level of different consumer groups (1 × TDF for primary consumer, 2 × TDF for secondary consumers etc.,) following Docmac *et al.* (2017). For invertebrate and zooplankton consumers we also included information on elemental composition (%C and %N) in the mixing model. Mean ($\pm$ SD) values were estimated from individual data but where these values were

not available, they were estimated from the literature for MOB (Stenzel *et al.* 2017) and POM (Rantala *et al.* 2021). The mixing model results were combined using an unweighted average approach across mean consumer contributions to calculate total contribution of each primary producer to the food web.

Given the likely existence of size-related differences in fish stable isotope values, we also used the *cosimmr* mixing model package (Govan *et al.* 2024) which allows the inclusion of covariates, using fish fork length as a covariate. In this case the prey items were used as sources and TDFs based on fish white muscle (mean $\pm$ SD: $\Delta^{13}C = 1.3 \pm 0.30$, $\Delta^{15}N = 2.9 \pm 0.32$) were used (McCutchan *et al.* 2003).

Isotopic niche width

The isotopic niche width of the perch population was quantified using the (*SIBER*) package in R (Jackson, Parnell & Jackson 2019). We calculated three common niche metrics: the total area (TA) of the convex hull, representing the overall range of $\delta^{13}C$ and $\delta^{15}N$ values; the standard ellipse area (SEA_B), which provides a bivariate measure of core isotopic niche space. Moreover, the niche size was also compared across size classes to inform the effect of growth of resource use.

Ethics statement

All sampling was conducted under Scottish Government netting license **CSM-25-114**. This study adheres to the ethical guidelines set by the University of Glasgow's Animal Welfare and Ethics Committee, ensuring that all sampling and handling procedures align with international standards for wildlife research and conservation. Gillnetting was carried out over a period of five weeks to prevent overfishing. Collected fish were euthanized using blunt force trauma, and no live specimens were transported to the

laboratory. All field data is securely stored in a shared OneDrive folder to maintain data protection. Ethics Application Reference: **EA18/25**.

Results (3138/1000-1500)

Limnological conditions

The lake showed pronounced thermal (Appendix A7) and oxygen stratification (Appendix A6) during the summer months, consistent with a monomictic mixing regime. In winter (October-February), surface water temperature ranged from 4.2℃ to 11.5℃, while bottom temperatures ranged between 4.0 and 8.4℃. The Lochan was ice-covered for several weeks between late December and early January. In summer (April-July), surface temperatures increased to 10.2℃ to 20.9 ℃, whereas bottom temperatures remained relatively stable, ranging between 7.0℃ to 8.2℃. The oxycline shifted seasonally, occurring at approximately 7 m depth in winter and rising to around 4 m in summer. Light attenuation was marked (Appendix A8), with an average Secchi depth of 2.25 m. The eutrophic depth (where 1% surface light remains) extended from ~3 m in winter to ~5 m in summer.

Headspace equilibrium test

***Table 1**. Mean ± concentration and stable isotope values recorded for CH4 and CO2 from different depths and areas of the Dubh Lochan during the current study. Note the spike in methane values at the bottom depths, especially at the deepest point 10 m.*

Site (maximum depth)	Depth	$[CH_4]$ (nM)	$[CO_2^+]$ (µM)	$\delta^{13}CH_4$ (‰)	$\delta^{13}CO_2$ (‰)
		(Mean ± SD)			
Central (10m)	Top	321.1 ± 5.3	16.0 ± 1.9	-32.0 ± 0.3	-10.6 ±0.2
	Middle	118.4 ± 38.2	153.9 ± 27.9	-11.00 ± 0.5	-21.7 ± 0.1
	Bottom	10697.0 ± 470.7	234.5 ± 9.1	-48.2 ± 14.8	-28.8 ± 0.3
North (6m)	Top	466.4 ± 171.6	17.9 ± 5.6	-69.6 ± 9.5	-21.6 ± 0.7
	Middle	382.8 ± 54.4	25.4 ± 1.9	-30.3 ± 0.4	-11.1 ± 0.1
	Bottom	172.0 ± 24.5	174.1 ± 39.3	-23.9 ± 0.1	-11.7 ± 0.5

Inlet (4m)	Top	270.1 ± 14.3	13.8 ± 2.8	-29.1 ± 0.3	-15.7 ± 0.8
	Middle	251.6 ± 4.3	17.5 ± 4.3	-30.3 ± 0.2	-9.9 ± 0.2
	Bottom	1931.0 ± 352.9	132.9 ± 97.8	-58.5 ± 16.8	-22.6 ± 0.2
Outlet (2m)	Top	340.1 ± 7.0	16.5 ± 3.2	-31.7 ± 0.3	-9.7 ± 0.2
	Middle	308.3 ± 33.7	12.9 ± 5.1	-30.9 ± 0.2	-14.6 ± 0.1
	Bottom	286.5 ± 19.5	19.6 ± 2.4	-30.1 ± 0.2	-12.6 ± 0.2

Concentrations of both CH_4 and CO_2 showed clear spatial and vertical variation in Dubh Lochan (Table 1). Across the four sites sampled, aqueous methane ($[CH_4]$) ranged from 118.4–10697.0 nM, with the highest values typically observed in the bottom layers. $\delta^{13}CH_4$ values averaged -34.5 ± 17.0‰, indicative of microbial methane production and oxidation. Dissolved CO_2 ($[CO_2^+]$) varied from 12.9–234.5 µM, with $\delta^{13}CO_2$ values between -28.8 and -9.7 ‰, showing modest vertical gradients.

Community structure

Although not assessed quantitatively, the macrophytes community of Dubh Lochan was dominated by *Phragmites spp.,* which were distributed all along the lochan's perimeter. The most visually abundant macrophytes following *Phragmites* were the water lilies *Nuphar luteum* and *Nymphea alba*, both of which were common in the littoral zone and extended into extended into surface waters over deeper areas (6-8 m depth), most prominently in the southern sector, extending into the 10 m zone adjacent to the peninsula. Submerged *Potamogeton spp*. were also abundant along the southern and northern arcs of the Lochan, particularly near the southern basin (close to the jetty).

The crustacean zooplankton assemblage in the pelagic zone was dominated by the omnivorous copepod *Eudiaptomus gracilis*, followed by the herbivorous species *Holopedum gibberum* and *Ceriodaphnia reticulate*. In the littoral zone, several herbivorous cladocerans were recorded, including *Daphnia hyalina*, *Bosmina coregoni*, and *C. reticulate*. The predatory cladcoceran *Polyphemus pediculus* and

predatory/detritivorous copepod *Mesocyclops leuckarti* were also recorded, but were restricted to littoral habitats.

The freshwater invertebrate community included profundal, littoral, and pelagic taxa. The profundal assemblage was dominated by the typically detritivorous benthic bloodworms (*Family Chironomidae*), with the zooplanktivorous phantom midge larvae (*Family Chaoboridae*) also present. The littoral invertebrate fauna was dominated by omnivorous water boatmen (*Family Corixidae*), predatory water mites (*Family Hydracarina*), predatory common backswimmers (*Family Notonectidae*), surface-hunting water striders (*Family Gerridae*), predatory alderfly larvae (*Family Sialidae*), omnivorous whirligig beetle (*Family Gyrinidae*), and the scavenging, omnivorous amphipod (*Family Gammaridae*), and detritivorous water louse *Asellus aquaticus*. Occasional representatives of predatory benthic and water column club-tailed dragonfly nymph *Gomphus vulgatissimus* and freshwater leech (*Family Piscicolidae*), as well as members of the orders of dragonflies (*Order Anisoptera*), damselfies (*Order Zygoptera*), and herbivorous caddisflies (*Order Trichoptera*) were observed. The pelagic invertebrate community was dominated by *Chaoboridae* larvae, with occasional individuals of *Families Gerridae* and *Gyrinidae* recorded in surface waters over depths of ~6-8 meters. Individuals from two species of primarily terrestrial but water-dependent invertebrates, such as the predatory orb-weaver spider (*Family Tetragnathidae*) and the largely herbivorous red-legged shieldbug (*Family Pentatomidae*) were also collected to compare isotopic values between the terrestrial and aquatic habitats. Reed beetles (*Family Chrysomelidae*) that use *N. luteum* and *N. alba* as structures to feed were also sampled.

Fish sampling indicated that Dubh Lochan supports a simple fish community composed of only two species which were apparently relatively abundant: perch, comprised 86.7 % of the survey catch by number and 17.9 % by biomass, and pike, comprising 13.3 % of the catch by number but 82.1 % by biomass.

Perch population structure

Sex

The overall sex ratio of immatures to females to male perch in the sample was approximately 2.8:2:1. A Chi-square goodness-of-fit test indicated that the proportion of females, immatures, and males in the sampled perch population differed significantly from an equal distribution ($\chi^2_{(2)} = 18.81$, $p < 0.001$). Immature individuals were the most abundant ($n = 62$), followed by females ($n = 44$) and males ($n = 22$). When examined seasonally, the sex ratio shifts from 1.7:1.1:1 in the winter ($n = 76$) to 14:12:1 in the summer ($n = 54$) ($\chi^2_{(2)} = 12.86$, $p = 0.0016$).

Length/mass differences

Perch length at 50% maturity was 99 mm (Appendix A3). The distribution of fork length (FL) was assessed for normality using Shapiro-Wilk tests, which indicated approximate normality for males ($W = 0.92$, $p = 0.079$) but slight deviation from normality for females ($W = 0.94$, $p = 0.048$). Given this, both parametric and non-parametric tests were performed to compare FL between males and females. A Welch two-sample t-test revealed a significant difference in mean FL between sexes ($t = 4.41$, $df = 46.19$, $p < 0.001$), with females (mean $\pm$ SD $= 159 \pm 49$) being larger than males (mean $\pm$ SD $= 106 \pm 42$). The 95% confidence interval for the difference in means was

29 to 77 mm. This finding was corroborated by a Wilcoxon rank-sum test ($W = 665.5$, $p < 0.001$), which also indicated significant difference in median FL between the sexes.

Similarly, body mass differed significantly between sexes. Both males ($W = 0.82$, $p = 0.002$) and females ($W = 0.8$, $p < 0.001$) deviated from normality for mass, prompting the use of both parametric and non-parametric tests. The Welch two-sample t-test showed a significant difference in mean mass (females: 73.2 ± 68.5 g; males: 23.3 ± 24.6 g; $t = 4.13$, $df = 54.2$, $p < 0.001$). A Wilcoxon rank-sum test confirmed this difference ($W = 671$, $p = 0.00014$), reinforcing that females are substantially heavier than males.

Mass-length relationship (allometric)

Based on Log-10 transformed data, the mass-length relationship for the European perch was well described by the model $M = aL^b$ with parameters $a = 4.42 \times 10^{-6}$ and $b = 3.22$ ($R^2 = 0.986$, SE of $b = 0.0357$), where M is estimated mass, L is fork length, a is the intercept parameter related to body form, and b is the allometric scaling exponent describing how mass changes with length. The scaling exponent b suggests slightly positive allometric growth.

An analysis of covariance (ANCOVA) (Table 2) comparing models with and without sex were both insignificant, indicating that the mass-length relationship did not differ significantly between males and females. Therefore, data from both sexes were pooled for the overall mass-length model.

Table 2. *ANOVA comparing the fit of two models predicting log-transformed mass from log-transformed length without (Model 1) and with sex (Model 2) as a predictor.*

Model	Residual df	RSS	df	Sum of squares	F	p-value
$log_{10}M \sim log_{10}L$	116	0.70919	-	-	-	-
$log_{10}M \sim log_{10}L \times Sex$	112	0.66812	4	0.04107	1.7212	0.1503

Stomach content analysis

Most perch had consumed prey immediately prior to capture with 18.5% of individuals having empty stomachs. Perch consumed a relatively limited range of prey with only nine main categories (Table 3). The most abundant prey consumed in terms of volume (mean $\%P_i = 28.4\%$) was *Chaoboridae spp.* larvae followed by *Sialidae spp.* larvae (19.6%) and *Chironomidae spp.* pupae (14.0%). Minor (<10% by volume) contributions were made by *Perca fluviatilis* (mean $\%P_i = 7.4\%$) and *Gomphidae spp.* larvae (mean $\%P_i = 5.0\%$). No crustacean zooplankton species were recorded from perch stomachs. Cannibalism was recorded in 7.8% of perch and cannibalistic individuals varied in size between 74 and 261 mm. The skeletons of consumed perch had estimated lengths varying between 20 and 64 mm.

Table 3. *Population level estimates of perch diet, including the mean numbers of prey per stomachs containing prey, the mean% contribution by volume (%Pi) and the frequency of occurrence (%FO)-the % of stomachs containing each prey category.*

Prey item	Average counts	Mean $\%P_i$	%FO	Notes
Chaoboridae spp. larvae	7.5	28.4	43.4	Most common prey
Chironomidae spp. larvae	4.4	21.5	31.0	
Chironomidae spp. pupae	2.9	14.0	11.6	
Sialidae spp. larvae	0.8	19.6	24.0	
Gomphidae spp. larvae	0.2	6.7	11.6	

Asellus aquaticus	0.1	1.7	2.3	
Ephemeroptera spp. larvae	0.02	0.5	1.6	
Gyrinidae spp. larvae	0.01	0.2	0.8	
Perca fluviatilis	0.09	7.4	7.8	Cannibalism

A PERMANOVA analysis comparing the diet of 'small (46 to 66 mm)', 'medium (70 to 126 mm)' and 'large (128 to 271 mm)' perch provided evidence for size-based differences in diet ($F_{(2, 92)} = 2.71$, $p = 0.0005$). A similar pattern was apparent for a comparison based on maturity classes ($F_{(2, 85)} = 2.13$, $p = 0.0084$). For size classes, SIMPER analysis showed that *Chaoboridae spp.* larvae were the most abundant prey item, with mean counts of approximately 13 individuals in small and medium individuals compared to 6 in large individuals. Larger-bodied *Sialidae spp.* larvae also contributed notably, with approximate mean counts of 1 individual in small perch, 1 in medium perch and 2 in larger perch. *Perca fluviatilis* prey were absent in the stomachs of the smallest perch, but averaged 0.1 individuals per consumer in medium perch, and 0.2 in large perch. *Asellus aquaticus* were present in low counts (0.2 individuals per stomach) but only in large perch. Other prey such as *Chironomidae spp.* larvae and pupae, *Anisoptera spp.*, *Ephemeroptera spp.*, and *Gyrinidae spp.* occurred at lower average counts across size classes.

Regarding maturity classes, *Chaoboridae spp.* larvae were again dominant with mean counts of ca. 6 individuals in young-of-year (YOY), of 16 individuals in juveniles, and 5 in adults. *Chironomidae spp.* larvae were also common with average counts of 2 (YOY), 9 (juveniles) and 1 (adults). Alderfly *Sialidae spp.* larvae had mean counts of 0.09 (YOY), 2 (juveniles), and 1 (adults). *Perca fluviatilis* prey were absent in YOY fish, but

were present in larger amounts in juvenile fish (0.24) than adults (0.12). Other prey items such as *Chironomidae spp.* pupae, *Gomphidae spp.*, *Asellus aquaticus*, *Ephemeroptera spp.*, and *Gyrinidae spp.* were present at low average counts without significant differences across maturity classes.

Stable isotope analysis

The isotopic composition of the Dubh Lochan (Fig. 5) exhibited a wide range of values (see Appendix A1). Basal sources in the system for $\delta^{13}C$ ranged from -32.6‰ to -26.0‰ ($range_{\delta 13C} = 6.67‰$) and from -4.9‰ to 3.3‰ ($range_{\delta 15N} = 8.2‰$) for $\delta^{15}N$. Consumers in Dubh Lochan spanned an even broader range; $\delta^{13}C$ values ranged between -37.7‰ and -24.7‰ ($range_{\delta 13C} = 13.0‰$) and $\delta^{15}N$ values between -4.9‰ and 10.2‰ ($range_{\delta 15N} = 15.1‰$), however, these ranges exclude methanotrophic bacteria (MOB). The low $\delta^{15}N$ values are indicative of the system's the nutrient concentration. Notably, zooplankton samples exhibited unexpected variation: *Eudiaptomus gracilis* occupied a relatively high trophic position ($\delta^{15}N_{mean}$: 6.8‰), whereas *Ceriodaphnia reticulate* had a lower $\delta^{15}N$ (mean: -2.3‰) than basal sources. This suggests the presence of a basal source not captured in our sample species, potentially phytoplankton.

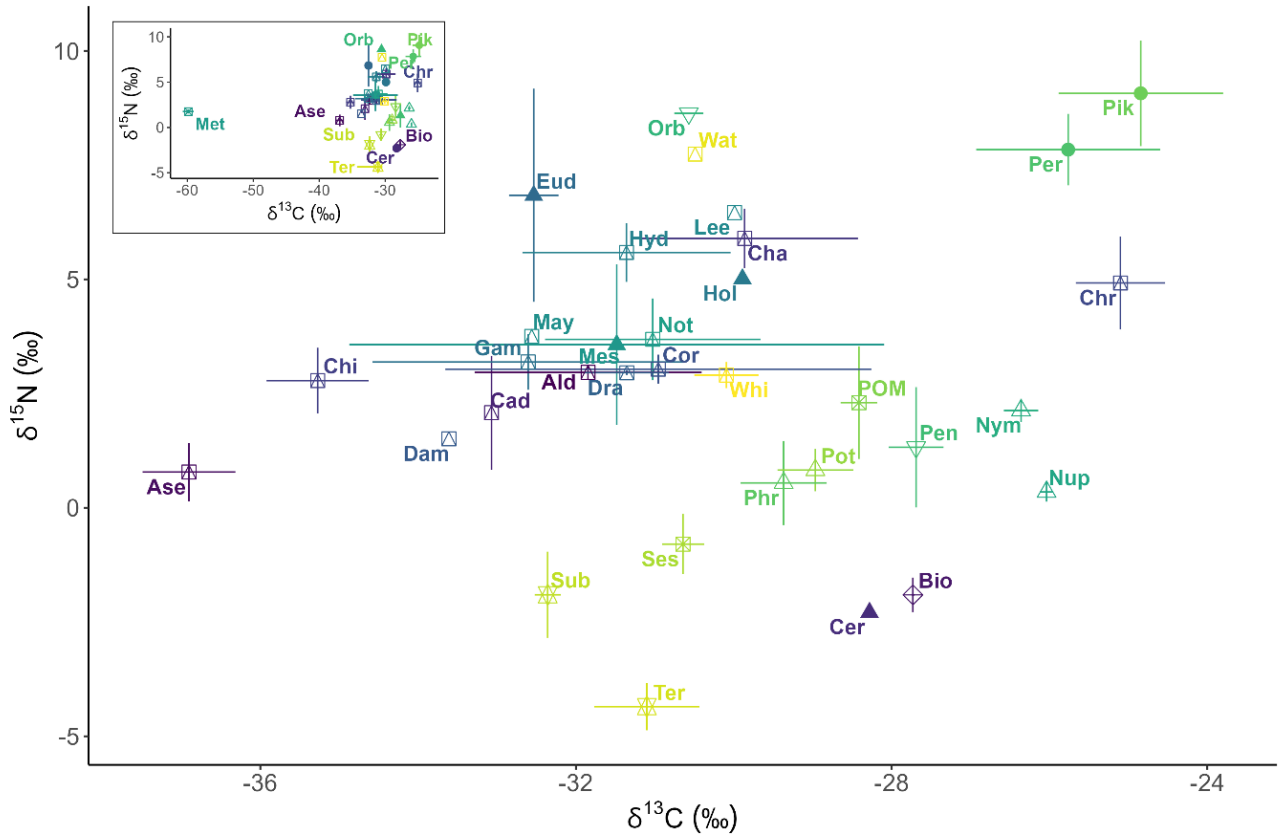

Figure 5. *Isotopic biplot depicting mean (± SD) $\delta^{13}C$ and $\delta^{15}N$ values for members of the Dubh Lochan community. The inset illustrates the literature-based ^{13}C-depleted estimates for methane-oxidising bacteria (MOB;* ***Met****) values relative to field-collected sources. Symbols denote functional groups and taxa: biofilm (rhomboid;* ***Bio****); macrophytes (triangles) – Nuphar alba (****Nup****), Nymphaea lutea (****Nym****), Phragmites spp. (****Phr****), Potamogeton spp. (****Pot****); leaf litter (overlapping upright and inverted triangles) – submerged (****Sub****), terrestrial (****Ter****); organic matter (cross within square) – particulate organic matter (****POM****), seston (****Ses****); zooplankton (solid triangles) – Ceriodaphnia reticulata (****Cer****), Eudiaptomus gracilis (****Eud****), Holopedium gibberum (****Hol****), Mesocyclops leuckarti (****Mes****); aquatic invertebrates (triangles within squares) – alderfly (****Ald****), Asellus aquaticus (****Ase****), caddisfly (****Cad****), Chaoboridae (****Cha****), Chironomidae (****Chi****), Chrysomelidae (****Chr****), Corixidae (****Cor****), damselfly (****Dam****), dragonfly (****Dra****), Gammaridae (****Gam****), Hydracarina (****Hyd****), leech (****Lee****), mayfly (****May****), Notonectidae (****Not****), water strider (****Wat****), whirligig beetle (****Whi****); terrestrial invertebrates (inverted triangles) – orb-weaver spider (****Orb****), Pentatomidae (****Pen****); fish (circles) – perch (****Per****), pike (****Pik****).*

Primary producers

Primary producers of the Lochan exhibited substantial variation in both $\delta^{13}C$ and $\delta^{15}N$ values ($range_{\delta 13C} = 34.0‰$, $range_{\delta 15N} = 7.2‰$), spanning from methane-oxidising bacteria (estimated $\delta^{13}C$: -60.0‰) to *Nuphar luteum* ($\delta^{13}C$: -26.0‰), and from terrestrial leaf litter ($\delta^{15}N$: -4.9‰) to particulate organic matter ($\delta^{15}N$: 2.3‰). Comparisons of leaf litter between samples collected from the forest floor and water-conditioned leaves from the lake littoral showed a shift in $\delta^{13}C$ from -31.1‰ in

terrestrial leaf litter to -32.4‰ in submerged leaves. There was a similar shift in $\delta^{15}N$ values which changed from -4.4‰ in dry terrestrial leaf litter to -1.9‰ in submerged terrestrial leaf litter. This shift provides evidence of trophic upgrading of leaf litter once the material enters the water.

Zooplankton

Zooplankton showed considerable variation in $\delta^{13}C$ values ($range_{\delta13C}$ = 7.9‰, $range_{\delta15N}$ = 12.1‰). From carbon values ranging between *Mesocyclops leuckarti* ($\delta^{13}C$: -35.2‰) and *Ceriodaphnia reticulata* ($\delta^{13}C$: -28.3‰) suggesting that the members were fuelled by distinct carbon sources, likely from varied production pathways (e.g. phytoplankton and methane-oxidising bacteria). The nitrogen values varied from *C. reticulata* ($\delta^{15}N$: -2.2‰) to *Eudiaptomus gracilis* ($\delta^{15}N$: 7.9‰) The major variation in $\delta^{15}N$ values indicated substantial differences in trophic position among the sampled zooplankton.

Aquatic, benthic and terrestrial invertebrates

Aquatic and benthic invertebrates exhibited a substantial variation in stable isotope values ($range_{\delta13C}$ = 13‰, $range_{\delta15N}$ = 7.7‰). The $\delta^{13}C$ values of these taxa ranged from *Asellus aquaticus* (-37.7‰) to reed beetle (*Family Chrysomelidae;* 24.7‰) and $\delta^{15}N$ values ranged from *A. aquaticus* (0.02‰) to water strider (*Family Gerridae;* 7.7‰). In contrast, terrestrial invertebrates had a relatively narrow $\delta^{13}C$ range ($range_{\delta13C}$ = 3.5‰) but a wider $\delta^{15}N$ range ($range_{\delta15N}$ = 8.2‰), spanning between red-legged shieldbug (*Family Pentatomidae;* $\delta^{13}C$: -27.3‰) and orb-weaver spider (*Family Tetragnathidae;* $\delta^{15}C$: -30.8‰) for $\delta^{13}C$ and between red-legged shieldbug (*Family Pentatomidae;* $\delta^{15}N$: 0.4‰) and orb-weaver spider (*Family Tetragnathidae;* $\delta^{15}N$: 8.6‰). The narrow $\delta^{13}C$ range among terrestrial taxa likely reflects the small sample size (only two species).

Fish

Fish stable isotope values were relatively uniform and showed expected ranges of both $\delta^{13}C$ (-33.7‰ to -28.3‰, $range_{\delta13C} = 5.4‰$) and $\delta^{15}N$ (5.3‰ to 10.2‰, $range_{\delta15N} = 4.9‰$) suggesting reliance on similar basal carbon sources across both fish populations (perch and pike) on similar basal sources. Perch, encompassed the $\delta^{13}C$ values of fish ranging from -33.7‰ to -28.3‰ ($range_{\delta13C} = 5.4‰$). The $\delta^{15}N$ values varied from 5.9‰ to 9.6‰ ($range_{\delta15N} = 3.7‰$) consistent with their generalist feeding strategy. This broad carbon range reflects variable habitat use and exploitation of multiple prey resources, while the variability in $\delta^{15}N$ indicates occupation of mid- to upper-trophic positions. In contrast, pike showed a narrower $\delta^{13}C$ range (-31.1 to -28.5‰; $range_{\delta13C}$= 2.6‰) and higher $\delta^{15}N$ values (7.6 to 10.2‰; $range_{\delta15N}$= 2.6‰), reflecting prey specialisation characteristic of apex predators that predominantly consume higher-trophic prey.

Mixing models output

We applied Bayesian isotope mixing models (*simmr*) to quantify the proportional contributions of ten primary (basal) and five secondary food sources to the diet of perch (*Perca fluviatilis*, $n = 127$) and pike (*Esox lucius*, $n = 10$) in Dubh Lochan. The ten basal sources comprised aquatic macrophytes (*Phragmites*, *Nymphaea*, *Nuphar*, *Potamogeton*), biofilm, submerged leaf litter, seston, particulate organic matter (POM), methane-oxidising bacteria (MOB), and terrestrial leaf litter. In addition, the relative contributions of different perch size classes to pike diet were modelled. Primary source contributions were also modelled for *A. aquaticus* ($n = 6$), Chironomidae ($n = 11$), and Chaoboridae ($n = 12$). Chaoboridae diets were further modelled for contributions from

six putative prey taxa (Chaoboridae, *Eudiaptomus gracilis*, *Holopedium gibberum*, and *Mesocyclops leuckarti*).

The six putative prey for perch and pike were *A. aquaticus*, Chaoboridae, *Sialidae*, and perch. For *Sialidae*, the seven secondary sources listed above were used. All source isotope values were adjusted for trophic discrimination using literature-derived trophic enrichment factors, and uninformative priors were applied in all models.

Perch

Posterior estimates (Table 4) indicated that perch were primarily fuelled by basal sources dominated by terrestrial leaf litter (median = 17.8 %), biofilm (13.1 %), followed by submerged leaf litter (9.3 %), and seston (7.8 %), with lower contributions from macrophytes and minimal assimilation of MOB (1.9 %). Credible intervals were narrow for MOB, reflecting strong isotopic separation, but broader for macrophytes, suggesting potential isotopic overlap and dietary flexibility. The putative prey contributions were dominated by Chaoboridae (median = 37 %), followed by Sialidae (18 %) and perch (15 %). The deviance from benthic prey (which use methane-derived carbon like chironomids) explains the low assimilation of carbon from methane-oxidising bacteria.

Table 4. *Stable isotope mixing model–derived estimates of dietary contributions from primary producers and secondary consumers to perch. Values are reported as medians with 95% Bayesian credible intervals (CrI), alongside means and standard deviations (SD).*

Type	Source	Median	95% CrI (Lower–Upper)	Mean	SD
Primary producer	*Biofilm*	0.13	0.01–0.56	0.18	0.15
	Phragmites	0.07	0.01–0.31	0.09	0.08
	Nymphea	0.05	0.01–0.17	0.06	0.04
	Nuphar	0.06	0.01–0.22	0.08	0.06
	Potamogeton	0.07	0.01–0.32	0.09	0.08
	Detritus plant matter	0.09	0.01–0.35	0.12	0.10
	Seston	0.08	0.01–0.43	0.11	0.11

	Methane-oxidising bacteria	0.02	0.01–0.04	0.02	0.01
	POM	0.05	0.01–0.20	0.07	0.05
	Terrestrial leaf litter	0.18	0.01–0.38	0.18	0.11
Putative prey	*Asellus*	0.08	0.02–0.19	0.09	0.05
	Chironomidae	0.09	0.02–0.21	0.09	0.05
	Chaoboridae	0.37	0.06–0.66	0.35	0.17
	Sialidae	0.18	0.03–0.52	0.20	0.13
	Perch	0.15	0.04–0.32	0.17	0.08
	Zooplankton	0.09	0.02–0.24	0.10	0.06

Mixing model with covariate (fork length)

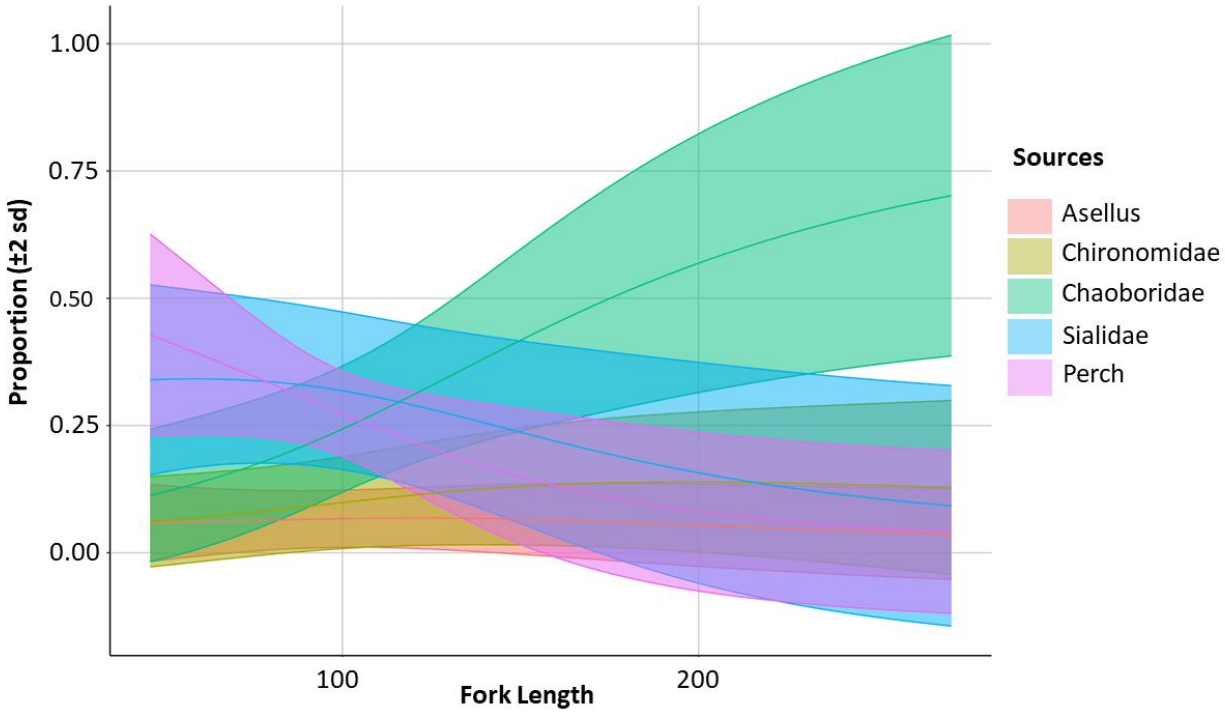

Figure 4. *Relationship between fork length of perch (Perca fluviatilis) and proportional contributions of dietary sources (Asellus, Chironomidae, Chaoboridae, Sialidae, Perch) estimated from cosimmr. The model indicates that the contributions of Chaoboridae to perch diet increases with size, while the contribution of conspecifics (perch) decreases.*

The *cosimmr* (Govan *et al.* 2024) model including fork length as a continuous covariate indicated marked changes in diet composition with increasing size (Figure 4). At the mean fork length, median dietary contributions (95% credible intervals) were: perch 41.2% (24.2–58.8%), Sialidae 33.8% (17.5–51.9%), Chaoboridae 11.1% (3.3–28.2%),

Chironomidae 5.3% (1.4–17.9%), and Asellus 5.2% (1.4–14.9%). Incorporating fork length as a continuous covariate revealed marked ontogenetic shifts. At smaller fork lengths, perch (mean = 37.3%, SD = 7.1%) and Sialidae (34.1 ± 8.4%) dominated the diet, with Chaoboridae contributing 15.1 ± 6.5%. At intermediate fork lengths, Chaoboridae increased to 33.2 ± 7.1% while perch declined to 20.2 ± 5.3% and Sialidae to 28.0 ± 8.1%; Chironomidae increased modestly to 11.7 ± 5.1%. At the largest fork lengths, Chaoboridae dominated (70.2 ± 15.8%), with all other prey contributing <13% (perch 4.1 ± 8.0%) (Table 5).

A loess smooth-plot for $\delta^{13}C$ (Appendix A11) and $\delta^{15}N$ (Appendix A12) was plotted to visualize the change in diet with size.

Table 5. *Posterior dietary proportions estimated from the cosimmr mixing model with fork length as a covariate. For the mean fork length, values represent the posterior median (95% credible intervals) and means (± SD). For small, medium, and large fork lengths, values represent posterior median (95% credible intervals). Results indicate a decline in perch contribution and an increase in Chaoboridae contribution increasing fork lengths.*

Prey item	Mean (± SD) contribution for size class			Contribution at mean fork length	
	Small	Medium	Large	Mean (± SD)	Median (95% CrI)
Asellus	0.06 (± 0.03)	0.07 (± 0.03)	0.04 (± 0.04)	0.06 (± 0.04)	0.05 (0.01 – 0.15)
Chironomidae	0.07 (± 0.04)	0.12 (± 0.05)	0.13 (± 0.09)	0.07 (± 0.04)	0.05 (0.01 – 0.18)
Chaoboridae	0.15 (± 0.07)	0.33 (± 0.07)	0.70 (± 0.16)	0.12 (± 0.07)	0.11 (0.03 – 0.28)
Sialidae	0.34 (± 0.08)	0.28 (± 0.08)	0.09 (± 0.12)	0.34 (± 0.09)	0.34 (0.18 – 0.52)
Perch	0.37 (± 0.07)	0.20 (± 0.05)	0.04 (± 0.08)	0.41 (± 0.09)	0.41 (0.24 – 0.59)

Pike

Table 6. *Estimated proportional contributions of basal sources, secondary producers, and perch size classes to pike diet based on stable isotope mixing models. Values are presented as medians with 95% Bayesian credible intervals (CrI), along with means and standard deviations (SD).*

Type	Source	Median	95% CrI (Lower–Upper)	Mean	SD
Primary producer	*Biofilm*	0.07	0.01–0.41	0.10	0.11
	Phragmites	0.05	0.01–0.31	0.08	0.10
	Nymphea	0.04	0.01–0.22	0.06	0.06
	Nuphar	0.05	0.01–0.24	0.07	0.07
	Potamogeton	0.05	0.01–0.30	0.08	0.08
	Detritus plant matter	0.09	0.01–0.47	0.13	0.13
	Seston	0.06	0.01–0.41	0.10	0.11
	Methane-oxidising bacteria	0.03	0.01–0.07	0.03	0.02
	POM	0.04	0.01–0.24	0.07	0.06
	Terrestrial leaf litter	0.21	0.01–0.83	0.30	0.25
Putative prey	*Asellus*	0.08	0.01–0.25	0.09	0.06
	Sialidae	0.22	0.03–0.52	0.23	0.14
	Small perch	0.21	0.03–0.54	0.21	0.14
	Medium perch	0.18	0.02–0.56	0.15	0.12
	Large perch	0.11	0.02–0.46	0.15	0.12
	Pike	0.06	0.01–0.34	0.09	0.09

Model (Table 6) estimates identified terrestrial leaf litter as the most prominent basal source (median contribution = 21%). Among prey items, Sialidae (22%) and small perch (21%) contributed most to the pike diet, followed by medium (18%) and large perch (11%). The strong representation of perch in the diet likely reflects prey specialization and size-based selectivity characteristic of pike feeding ecology. However, interpretation of these estimates is constrained by the limited sample size, which may have reduced model precision.

Chironomidae

Mixing models (Table 8) indicated that chironomid larvae were mostly fuelled by methane-oxidising bacteria (median = 15.3 %), followed by terrestrial leaf litter

(median = 13.4 %) and submerged leaf litter (11.4 %). Biofilm (median = 9.8 %) and the macrophytes do not play as important a role.

***Table 7**. Estimated proportional contributions of different basal sources to chironomid diets based on stable isotope mixing models. Values are presented as medians with 95% Bayesian credible intervals (CrI), along with means and standard deviations (SD)*

Source	Median	95% CrI (Lower–Upper)	Mean	SD
Biofilm	0.01	0.01–0.50	0.14	0.13
Phragmites	0.05	0.01–0.19	0.06	0.05
Nymphea	0.03	0.01–0.15	0.05	0.04
Nuphar	0.04	0.01–0.17	0.05	0.04
Potamogeton	0.04	0.01–0.18	0.06	0.05
Detritus plant matter	0.11	0.01–0.52	0.16	0.14
Seston	0.07	0.01–0.41	0.11	0.11
Methane-oxidising bacteria	0.15	0.12–0.19	0.15	0.02
POM	0.04	0.01–0.15	0.05	0.04
Terrestrial leaf litter	0.13	0.01–0.50	0.17	0.14

Chaoboridae

Mixing models (Table 9) indicated that terrestrial leaf litter contributed most to *Chaoboridae* somatic mass (median = 0.20, 95 % CrI: 0.02–0.47), while methane-oxidising bacteria contributed least (0.03, 0.01-0.05). In terms of consumptive putative prey *Eudiaptomus* had the highest median contribution (0.28, 0.04–0.63), followed by Chaoboridae (0.21, 0.02–0.60) and *Holopedium* (0.18, 0.01–0.58), with *Ceriodaphnia* contributing the least (0.08, 0.01–0.25).

***Table 8.** Median proportional contributions (with 95% Bayesian credible intervals, means, and standard deviations) of primary and secondary producers to the diet of Chaoboridae, estimated using a stable isotope mixing model.*

Type	Source	Median	95% CrI (Lower–Upper)	Mean	SD
Primary producers	*Biofilm*	0.10	0.01–0.52	0.15	0.14
	Phragmites	0.06	0.01–0.29	0.09	0.08
	Nymphea	0.05	0.01–0.18	0.06	0.05
	Nuphar	0.06	0.01–0.23	0.07	0.06
	Potamogeton	0.06	0.01–0.28	0.08	0.07

	Detritus plant matter	0.10	0.01–0.46	0.14	0.13
	Seston	0.07	0.01–0.44	0.11	0.12
	Methane-oxidising bacteria	0.03	0.01–0.05	0.03	0.01
	POM	0.05	0.01–0.20	0.07	0.05
	Terrestrial leaf litter	0.20	0.02–0.47	0.21	0.13
Putative prey	*Mesocyclops*	0.15	0.02–0.43	0.17	0.11
	Chaoboridae	0.21	0.02–0.60	0.26	0.16
	Eudiaptomus	0.28	0.04–0.63	0.29	0.15
	Ceriodaphnia	0.08	0.01–0.25	0.09	0.06
	Holopedium	0.18	0.01–0.58	0.22	0.15

Asellus

The mixing model (Table 10) that methane-oxidising bacteria contributed the largest proportion to *A. aquaticus* diets (median = 22%, 95% CrI: 6–28%; mean ± SD = 21 ± 5%), with all other basal sources contributing more evenly at medians of 5–7% each. Detrital plant matter (median = 7%, 1–37%) and terrestrial leaf litter (7%, 1–36%) showed wide credible intervals, reflecting substantial uncertainty and possible isotopic overlap among basal sources. This pattern suggests that while *A. aquaticus* exhibits a generalist feeding mode, methane-derived carbon may play a notable role in its energy pathway.

Table 9. *Posterior estimates of proportional contributions of basal food sources to Asellus aquaticus diets in Dubh Lochan, based on Bayesian isotope mixing models (simmr). Values show median, 95% credible interval (CrI), mean, and standard deviation (SD) for each source. Methane-oxidising bacteria contributed most strongly to A. aquaticus energy intake, while other sources were more evenly distributed.*

Source	Median	95% CrI (Lower–Upper)	Mean	SD
Biofilm	0.07	0.01–0.35	0.10	0.09
Phragmites	0.06	0.01–0.28	0.08	0.07
Nymphea	0.05	0.01–0.25	0.07	0.07
Nuphar	0.06	0.01–0.26	0.07	0.07
Potamogeton	0.06	0.01–0.27	0.08	0.07
Detritus plant matter	0.07	0.01–0.37	0.11	0.10
Seston	0.07	0.01–0.35	0.10	0.09
Methane-oxidising bacteria	0.22	0.06–0.28	0.21	0.05
POM	0.06	0.01–0.25	0.08	0.06

Terrestrial leaf litter	0.07	0.01–0.36	0.10	0.10

Unweighted total contributions

When averaged across consumers (Table 10), the most important basal resources for the Lochan food web were terrestrial leaf litter (16.8 ± 6.3%), detrital plant matter (12.9 ± 5.2%), biofilm (13.4 ± 4.7%), and seston (10.6 ± 4.7%). Methane-oxidising bacteria, despite low assimilation in higher consumers, contributed substantially overall (8.8 ± 1.2%), reflecting their importance to benthic invertebrates. Individual macrophyte species (Nymphea, Nuphar, Potamogeton) contributed more modestly (≈6–8% each), but together accounted for ~20% of assimilated resources.

Table 10. *Estimated contributions (% mean ± SD) of basal sources to five representative consumers (perch, pike, Chaoboridae, Chironomidae, Asellus) in the Dubh Lochan, based on stable isotope mixing models (simmr). "Total contribution" values represent the mean (±SD) across all consumers, providing an integrative estimate of each source's overall importance to the Lochan food web.*

Source	Contributions to consumer taxon (%mean ± SD)					Total (%mean ± SD) contribution
	Perch	Pike	Chaoboridae	Chironomidae	Asellus	
Biofilm	17.8 ± 3.0	10.4 ± 10.9	14.7 ± 13.6	14.1 ± 13.0	9.8 ± 9.0	**13.4 ± 4.7**
Phragmites	8.9 ± 8.0	7.6 ± 7.6	8.5 ± 7.5	5.8 ± 5.1	8.0 ± 6.9	**7.8 ± 3.2**
Nymphea	6.0 ± 4.4	5.9 ± 5.9	5.9 ± 4.7	4.4 ± 3.6	7.2 ± 6.1	**5.9 ± 2.3**
Nuphar	7.8 ± 5.7	6.6 ± 6.4	7.4 ± 5.9	5.3 ± 4.7	7.3 ± 6.1	**6.9 ± 2.6**
Potamogeton	9.3 ± 8.1	7.8 ± 7.7	8.2 ± 7.2	5.7 ± 4.8	8.0 ± 6.9	**7.8 ± 3.2**
Detritus plant matter	12.0 ± 9.5	12.6 ± 12.6	14.0 ± 12.4	15.2 ± 13.2	10.6 ± 9.5	**12.9 ± 5.2**
Seston	11.4 ± 10.8	9.6 ± 10.7	11.3 ± 11.5	10.7 ± 10.1	10.2 ± 9.2	**10.6 ± 4.7**
Methane-oxidising bacteria	1.9 ± 0.1	3.4 ± 2.0	2.6 ± 1.2	15.5 ± 1.9	20.8 ± 4.7	**8.8 ± 1.2**
POM	6.8 ± 5.2	6.5 ± 6.3	7.0 ± 6.0	5.0 ± 4.2	8.0 ± 6.0	**6.7 ± 2.5**

Terrestrial leaf litter	18.1 ± 10.5	29.6 ± 24.7	21.0 ± 13.0	17.0 ± 14.0	10.5 ± 9.6	**19.2 ± 8.5**

Isotopic niche width

The perch community was first visualised in the form of SIBER ellipses (Appendix A13) and niche size comparison by size (Appendix A14). The community exhibited a total convex hull area (TA) of 14 ‰², with a standard ellipse area (SEA) of 2.69 ‰² (SEAc = 2.71), indicating a relatively constrained core isotopic niche. The Bayesian standard ellipse area (SEA_B) was 1.72 ‰² (95% CrI: 1.31–2.35) for small perch, 2.86 ‰² (95% CrI: 2.14–3.95) for medium perch, and 2.36 ‰² (95% CrI: 1.76–3.25) for large perch. These values indicate a relatively narrow isotopic niche, smaller than that reported for perch in Lake Jyväsjärvi, Finland (TA = 31.7 ‰²; Syväranta *et al.* (2013)), suggesting reduced trophic diversity in Dubh Lochan population. To contextualise these findings, standard ellipse metrics were also compared across other lentic systems (Table 11), allowing evaluation of the perch population's relative isotopic niche size. Moreover, the niche size seemed to increase with body size in perch which reflects broader diet breadths.

Table 11. *Comparison of standard ellipse area metrics (SEA_B: Bayesian standard ellipse area, SEAc: corrected standard ellipse area) of perch (Perca fluviatilis) populations across European and Anatolian lake systems, including Dubh Lochan (current study). Values illustrate the relative trophic niche widths of perch in different lentic environments, with surface area and location provided where available.*

System	Surface area (km²)	SEA_B (median in ‰²)	SEA_c (in ‰²)	Source
Dubh Lochan, Scotland	<0.1	1.7	2.7	Current study
İznik Lake, Turkey	298	18.5	3.3	Tarkan *et al.* (2023)
Undisclosed lentic system from southern England	-	7.8	6.5	Kurtul, Tarkan and Britton (2023)

Lake Milada, Czech Republic	2.5	-	3.5	Vejříková *et al.* (2023)
Most Lake, Czech Republic	3.1	-	4.3	
Raha, Finland	22.9	-	2.6	Hayden, Harrod and Kahilainen (2014)
Vuontis, Finland	10.9	-	4.2	
Aksu, Finland	3.8	-	1.4	
Kivi, Finland	3.5	-	4.6	

Discussion (1142/2000-2500)

Our results provide key insights into carbon cycling and energy flow in the Dubh Lochan. The food web of this dystrophic system is sustained by a diverse suite of primary producers, each contributing in different ways to overall energy flow. Interestingly, of the primary producers were ^{15}N-depleted, indicating the low concentrations of dissolved inorganic nitrogen in the system. Moreover, some consumers, such as *Ceriodaphnia reticulata*, exhibited δ^{15}N values lower than any measured primary producers, suggesting the presence of an unaccounted basal resource, most probably phytoplankton, that was not captured in our sampling. As expected in a humic, nutrient-poor lake, terrestrial leaf litter contributes approximately 17% ($\pm$ 6.3) to the food web, with an additional ~13% from in-lake conditioned detrital leaf litter, whose role remains complicated (Guggenheim *et al.* 2020). Together, these sources account for ~30% of the food web energy. This places Dubh Lochan well within the range of other small, humic lakes, where terrestrial contributions to consumer biomass typically range from 30-94% depending on productivity and hydrological context (Cole *et al.* 2011; Zigah 2013; Tanentzap *et al.* 2017). Although our unweighted

estimates may underestimate total biomass contributions, the results underscore the centrality of allochthonous terrestrial carbon in sustaining this system.

In contrast, particulate organic matter appeared to play a relatively minor role (%mean relative contribution: 6.7% $\pm$ 2.5), likely reflecting the dystrophic character of the Lochan. Interestingly, although individual aquatic macrophyte taxa (e.g. *Phragmites* (7.8%), *N. luteum* (6.9%), *N. alba* (5.9%), and *Potamogeton* (7.8%)) showed limited contributions when considered separately, their combined input amounted to ca. 28.4% of the total energy base, comparable to the terrestrial contribution. This highlights that macrophytes collectively represent a major autochthonous subsidy to consumers, despite their seemingly modest individual roles. This can be supported by studies where terrestrial subsidies have been witnessed to drop to ca. 10% with elevated autochthonous production (Cole *et al.* 2011). The role of seston (10.6% $\pm$ 4.7), however, remains obscure due to uncertainty over its composition, which may include suspended lake sediments (Knowlton & Jones 2000), algal cells (Moss 1970), bacteria (Pennington & Tutin 1974), and fine detritus (Lenz 1977). Without this resolution, its quantitative contribution to consumer biomass cannot be clearly determined.

Along these basal resources, methane-oxidising bacteria (MOB) represent an important microbial source of carbon in the Dubh Lochan. Our models indicate that MOB make a measurable contribution to key benthic consumers such as chironomids and *Asellus aquaticus*, highlighting their role in funnelling methane-derived carbon into the food web. This microbial pathway provides a direct link between the chemical environment of the Lochan and higher trophic levels, setting the stage for a broader consideration of methane dynamics in water column. It is important to note that methane-oxidising bacteria (MOB) were not directly sampled in this study. Instead, we incorporated $\delta^{13}C$

and $\delta^{15}N$ values from the literature (Lau *et al.* 2014a) as representative end-members in our mixing models. While this approach provides a useful proxy, it introduces some uncertainty given potential site-specific variation in MOB isotopic signatures.

To place this potential pathway into context, we next consider the availability of methane in the Dubh Lochan water column. A striking and novel finding was the detection of high methane concentrations in the profundal, anoxic depths of the Lochan, marking the first evidence of methane in this system. Concentrations reached up to $10{,}697.0 \pm 470.7$ nM, strongly suggesting active methanogenesis, likely via acetoclastic or hydrogenotrophic pathways. Although lower than those reported from deep stratified systems such as Lake Lugano (150,000-260,000 nM; van Grinsven *et al.* (2020)), values are consistent with shallow humic lakes where methane is known to accumulate under oxygen-poor conditions (Laakso & Schrag 2019; Baliña *et al.* 2022). The isotopic composition of methane ($\delta^{13}CH_4$: -34.5‰) further supports a microbial origin, predominantly acetoclastic fermentation (Minick *et al.* 2019).

Despite this abundance, the incorporation of methane-derived carbon into higher trophic levels appeared limited. Several factors may explain this pattern: physiological constraints on consumers, inefficient trophic transfer, or direct atmospheric release via ebullition, bypassing the microbial bio-filter. Additionally, our use of proxy MOB values from Lau *et al.* (2014a) rather than direct sampling introduces uncertainty; if the isotopic signatures of local MOB differ substantially, their contribution to the food web may be underestimated. This highlights an important distinction between methane as a biogeochemical pool and its role in sustaining consumer biomass, a theme echoed in other shallow systems where methane cycling can be intense but only weakly coupled to higher trophic levels (Donis *et al.* 2017; Itoh *et al.* 2017).

Similarly, in the Dubh Lochan, our results indicate that methane cycling alone cannot explain energy transfer. Instead, our food web analysis further revealed the important role of benthic-pelagic linkages mediated by invertebrates. Chironomids, long recognised as key conduits of benthic energy into pelagic consumers (Wagner, Volkmann & Dettinger-Klemm 2012), were fuelled in our system by a mixture of methane-oxidising bacteria (15.5%), detrital plant matter (15.2%), and pelagic biofilm (14.1%). This suggests that while methane does contribute indirectly, Chironomids also rely on algal biofilms, consistent with their grazing behaviour (Tarkowska-Kukuryk 2013). Diatoms are often the dominant algal food source (McLachlan, Brennan & Wotton 1978; Cattaneo 1983; Tokeshi 1986), though cyanobacteria may also form an important component (Ali 1990). Future work quantifying species-specific chironomid diets could clarify their role in mediating energy transfer from multiple carbon pathways.

Chaoboridae, the pelagic primary prey of perch in the system, demonstrated a contrasting energy signature, with terrestrial leaf litter (21%) and biofilm (14.1%) representing their dominant carbon sources. This reliance on terrestrially derived material underscores the significance of cross-habitat subsidies in supporting higher trophic levels, further highlighting that methane-derived carbon alone cannot explain the energy pathway of the food web.

Similarly, the isotopic depletion observed in littoral *Asellus aquaticus* indicates a strong reliance on terrestrially derived detritus conditioned by methane-oxidising bacteria (20.8%). To our knowledge, this represents the first evidence of a littoral methane-cycling signal resulting in a depleted carbon-isotope value for *A. aquaticus*, raising the possibility that methane-linked trophic processes extend beyond profundal habitats

into shallow zones where terrestrial inputs are greatest. This edge effect, likely driven by transitions between woodland and humic-rich waters, represents a novel avenue for understanding littoral-profundal connectivity.

Beyond invertebrates, we observed cross-ecosystem energy transfer into terrestrial consumers. The predatory orb-weaver spider (*Family Tetragnathidae*) exhibited isotopic values indicative of reliance on aquatic prey, highlighting how lake-derived production can subsidise adjacent terrestrial food webs.

The case study of perch *Perca fluviatilis* provides a particularly interesting perspective. While perch are classically known to shift ontogenetically from planktivory to piscivory (Byström, Huss & Persson 2012), our isotope mixing models instead indicated an increasing reliance on Chaoboridae with body size. This contrasts with stomach content analysis (SIMPER) on key prey taxa, which suggested a declining contribution of Chaoboridae with size. Such discrepancies likely reflect methodological differences; isotope data integrates long-term assimilated diet (e.g. 6 months in muscle tissue (Thomas & Crowther 2015)), whereas stomach contents capture short-term feeding and may underrepresent soft-bodied prey such as Chaoboridae (Polito *et al.* 2011; Davis & Pineda Munoz 2016; Petta *et al.* 2020). Taken together, the results imply that Chaoboridae remain an important dietary component of perch over time, even if episodically replaced by other prey. Long-term monitoring across seasons would clarify how perch balance short-term opportunism with consistent energy assimilation.

Finally, our sampling revealed a skewed perch population dominated by females during the summer. This could be due to female-biased size dimorphism (Prchalová *et al.* 2022) which may have contributed to gear bias. Understanding these dynamics would

require focused behavioural studies that track perch movement and sex-specific foraging across seasons.

Conclusion (504/500)

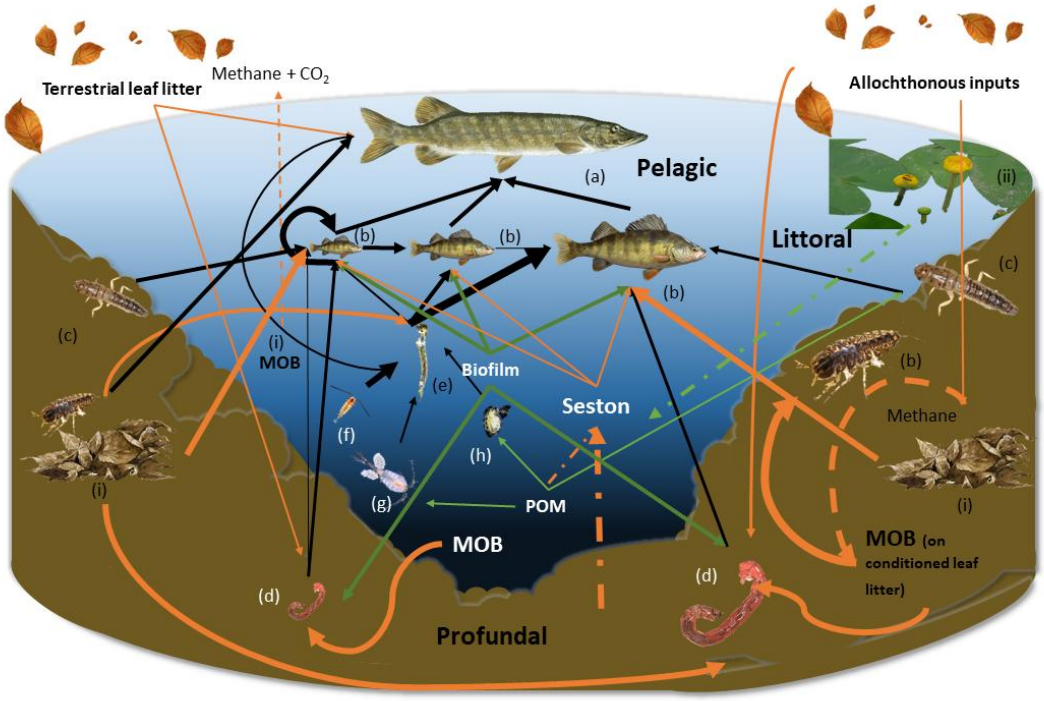

Figure 5. *Visual representation of the Dubh Lochan food web. Primary resources include (i) detrital organic matter (submerged leaf litter) and (ii) macrophytes (e.g., Nuphar luteum). Consumers include (a) pike, (b) perch of the three main size classes, (c) Sialidae, (d) chironomids, (e) Chaoboridae, and (f) Eudiaptomus gracilis. Arrows indicate the direction of energy flow from resource or prey to consumer, with thickness representing the relative magnitude of contribution (thicker arrows indicate higher contribution). Arrow colour denotes the primary production pathway: orange indicates terrestrial/detritus-fuelled energy, and green indicates photosynthetic primary production.*

Overall, the Dubh Lochan emerges as a system strongly subsidised by terrestrial carbon inputs, with methane cycling present but only weakly incorporated into the food web (see Figure 5). Benthic invertebrates such as chironomids and *Asellus aquaticus* form critical pathways linking terrestrial and microbial sources into pelagic consumers, while perch and even terrestrial predators such as orb-weaver spiders illustrate how these energy flows cascade through multiple trophic levels. These findings reinforce the view that dystrophic lakes are shaped by a complex interplay of terrestrial detritus, microbial

processes, and trophic interactions, and they highlight the need for future work integrating seasonal dynamics, behavioural ecology, and cross-ecosystem linkages.

The certainty of our results is constrained by the resolution of the methodologies employed. While bulk $\delta^{13}C$ and $\delta^{15}N$ values provide integrative insights into dietary sources and trophic positions, they cannot fully resolve overlapping carbon sources or microbial pathways (Besser, Elliott Smith & Newsome 2022; Heikkinen *et al.* 2022). Incorporating $\delta^{34}S$ (Fry *et al.* 1986; Connolly *et al.* 2004; Sayle *et al.* 2013) and $\delta^{2}H$ (Karlsson *et al.* 2012) alongside $\delta^{13}C$ and $\delta^{15}N$ would improve discrimination between methane- and photosynthesis-derived carbon, while compound-specific stable isotope analysis (CSIA) of fatty acids or amino acids could clarify key biochemical pathways. Coupling these isotopic approaches with direct methane flux measurements (Natchimuthu *et al.* 2016; Itoh *et al.* 2017), microbial community sequencing (Beck *et al.* 2013; He *et al.* 2015; Cadieux *et al.* 2022), and expanded spatial and temporal sampling (Natchimuthu *et al.* 2016; Kang, Liu & Grossart 2024) would substantially enhance resolution. Sampling across stratification cycles, ice cover, and hydrological variation would also capture seasonal dynamics of methane cycling and its incorporation into the food web.

Future research could explore several complementary avenues. Revisiting the perch population structure in Dubh Lochan, particularly in comparison to Shafi (1969) and Shafi and Maitland (1971), would reveal whether changes in basal resources or prey availability have altered trophic dynamics over time.

Furthermore, spatially-targeted methane-focused analyses along the littoral zone would determine whether invertebrates are consistently methane-fuelled along the shoreline or whether areas such as the southern end near the jetty create localized hotspots for

methane cycling. Temporal studies incorporating perch diet and isotope analysis across different tissues throughout the year would provide more representative $\delta^{13}C$ and $\delta^{15}N$ signals, capturing seasonal shifts in resource use and episodic methane incorporation.

Summing up, this places the Dubh Lochan (located near the Scottish Centre for Ecology and the Natural Environment) at an ideal location for long-term ecological research (LTER) frameworks integrating stable isotopes, molecular biology, biogeochemical measurements (Magnuson 1990). This will aid in ecosystem modelling, which will be essential for predicting how dystrophic lake ecosystems respond to environmental change, including climate warming (Havens & Jeppesen 2018), stratification shifts (Woolway *et al.* 2021), and catchment land-use alterations (Fraterrigo & Downing 2008). Warmer conditions can disproportionately accelerate microbial methanogenesis relative to methane oxidation, particularly in littoral sediments, leading to episodic methane accumulation and release (James *et al.* 2016; Yang *et al.* 2023). Comparative studies across lakes differing in trophic status, methane production, and hydrological regimes will allow broader generalisations and identification of key drivers influencing methane incorporation into food webs.

Collectively, these approaches will advance our understanding of energy flow in dystrophic lakes, highlighting the nuanced roles of methane cycling, microbial chemosynthesis, and terrestrial subsidies in supporting aquatic food webs. Integrating behavioural ecology with isotopic and microbial analyses offers a promising avenue for elucidating how predator foraging strategies adapt to resource availability and environmental constraints (Yeakel *et al.* 2016b; Dhellemmes *et al.* 2021; Grainger *et al.* 2023), paving the way for predictive and conservation-focused ecological insights.

Acknowledgments (237/250)

This project and its outcomes have been the result of the support and encouragement of many well-wishers. First and foremost, I would like to thank Prof. Chris Harrod for being an incredible supervisor throughout the duration of the project. His invaluable insights and contagious enthusiasm were key to the successful completion of this ambitious work. I would also like to thank James Milton for his support in the field and beyond. Without James's help, I would have missed out on valuable data, opportunities and his lovely camaraderie.

I am grateful to the Scottish Centre for Ecology and the Natural Environment (SCENE) for providing the necessary infrastructure and logistical support to carry out this project. I would also like to thank Prof. Darren Gröcke for his invaluable and unconditional support in analysing the stable isotope samples; Dr. Adrian Bass and Kenny Roberts for lending us the Ekman grab and allowing us to conduct the methane analysis at their facility; and Prof. Colin Adams for permitting the use of his fishing nets and minnow traps. I would also like to extend my sincere gratitude to Eden Pennycott, Eiryn Milligan, Emily Stewart, Hannele Honkanen, Isaac Westlake, Kieran Killen, Maddie Inglis, Phoebe Kaiser-Wilks, and Zoe Riemersma for all their help and encouragement. Finally, I would like to thank my family (Mumma, Dadda, and Keyur) for enduring the uncertainties of my missing calls and for being my backbone over the past year.

Bibliography

Aberle, N. & Malzahn, A.M. (2007) Interspecific and nutrient-dependent variations in stable isotope fractionation: experimental studies simulating pelagic multitrophic systems. *Oecologia,* **154,** 291-303.

AFSC (2015) *Resource ecology and ecosystem modeling stomach content analysis procedures manual*. AFSC, Seattle.

Ali, A. (1990) Seasonal changes of larval food and feeding of Chironomus crassicaudatus (Diptera: Chironomtdae) in a subtropical lake.

Amblard, C., Jean-François, C., Bourdier, G. & Maurin, N. (1995) The microbial loop in a humic lake: seasonal and vertical variations in the structure of the different communities. *Hydrobiologia,* **300-301,** 71-84.

Armour, K., Forster, P., Storelvmo, T., Collins, W., Dufresne, J.-L., Frame, D., Lunt, D., Mauritsen, T., Palmer, M. & Watanabe, M. (2021) The Earths energy budget, climate feedbacks, and climate sensitivity. *AGU Fall Meeting Abstracts*, pp. U13B-07.

Assessment, M.E. (2005) *Ecosystems and human well-being: wetlands and water*. World resources institute.

Baliña, S., Bernal, M., Sánchez, M. & Giorgio, P. (2022) *Methane production in the oxic water column of shallow lakes from the Pampean Plain with different alternative regimes*.

Barber, T.R., Burke Jr, R.A. & Sackett, W.M. (1988) Diffusive flux of methane from warm wetlands. *Global Biogeochemical Cycles,* **2,** 411-425.

Bastviken, D., Tranvik, L.J., Downing, J.A., Crill, P.M. & Enrich-Prast, A. (2011) Freshwater Methane Emissions Offset the Continental Carbon Sink. *SCIENCE,* **331,** 50-50.

Beck, D.A., Kalyuzhnaya, M.G., Malfatti, S., Tringe, S.G., Glavina Del Rio, T., Ivanova, N., Lidstrom, M.E. & Chistoserdova, L. (2013) A metagenomic insight into freshwater methane-utilizing communities and evidence for cooperation between the Methylococcaceae and the Methylophilaceae. *PeerJ,* **1,** e23.

Belle, S. & Cabana, G. (2020) Effects of changes in isotopic baselines on the evaluation of food web structure using isotopic functional indices. *PeerJ,* **8,** e9999.

Bergström, A.K. & Jansson, M. (2000) Bacterioplankton Production in Humic Lake Örträsket in Relation to Input of Bacterial Cells and Input of Allochthonous Organic Carbon. *Microbial Ecology,* **39,** 101-115.

Besser, A.C., Elliott Smith, E.A. & Newsome, S.D. (2022) Assessing the potential of amino acid δ13C and δ15N analysis in terrestrial and freshwater ecosystems. *Journal of Ecology,* **110,** 935-950.

Bogard, M.J. & del Giorgio, P.A. (2016) The role of metabolism in modulating CO2 fluxes in boreal lakes. *Global Biogeochemical Cycles,* **30,** 1509-1525.

Burian, A., Nielsen, J.M., Hansen, T., Bermudez, R. & Winder, M. (2020) The potential of fatty acid isotopes to trace trophic transfer in aquatic food-webs. *Philosophical Transactions of the Royal Society B,* **375,** 20190652.

Byström, P., Huss, M. & Persson, L. (2012) Ontogenetic constraints and diet shifts in Perch (Perca fluviatilis): mechanisms and consequences for intra-cohort cannibalism. *Freshwater Biology,* **57,** 847-857.

Cadieux, S.B., Schütte, U.M.E., Hemmerich, C., Powers, S. & White, J.R. (2022) Exploring methane cycling in an arctic lake in Kangerlussuaq Greenland using stable

isotopes and 16S rRNA gene sequencing. *Frontiers in Environmental Science,* Volume 10 - 2022.

Carpenter, S.R., Stanley, E.H. & Vander Zanden, M.J. (2011) State of the World's Freshwater Ecosystems: Physical, Chemical, and Biological Changes. *Annual Review of Environment and Resources,* **36,** 75-99.

Cattaneo, A. (1983) Grazing on epiphytes 1. *Limnology and Oceanography,* **28,** 124-132.

Cole, J.J., Carpenter, S.R., Kitchell, J., Pace, M.L., Solomon, C.T. & Weidel, B. (2011) Strong evidence for terrestrial support of zooplankton in small lakes based on stable isotopes of carbon, nitrogen, and hydrogen. *Proc Natl Acad Sci U S A,* **108,** 1975-1980.

Cole, J.J., Prairie, Y.T., Caraco, N.F., McDowell, W.H., Tranvik, L.J., Striegl, R.G., Duarte, C.M., Kortelainen, P., Downing, J.A. & Middelburg, J.J. (2007) Plumbing the global carbon cycle: integrating inland waters into the terrestrial carbon budget. *Ecosystems,* **10,** 172-185.

Connolly, R.M., Guest, M.A., Melville, A.J. & Oakes, J.M. (2004) Sulfur stable isotopes separate producers in marine food-web analysis. *Oecologia,* **138,** 161-167.

Coyne, J., Connor, L. & Kelly, F. (2019) *Manual for Ageing Common Freshwater Fish Species in Ireland. IFISH Fish and Habitats: Science and Management Vol. 1*.

Crim, L.W.G., B. D. (1990) Reproduction. *Methods For Fish Biology* (ed. C.B.S.P.B. Moyle), pp. 529 - 553. American Fisheries Society, Bathesda, Maryland.

Croft, P. (1986) A key to the major groups of British freshwater invertebrates. *Field studies,* **6,** 531-579.

Davis, M. & Pineda Munoz, S. (2016) The temporal scale of diet and dietary proxies. *Ecol Evol,* **6,** 1883-1897.

de Kluijver, A., Schoon, P.L., Downing, J.A., Schouten, S. & Middelburg, J.J. (2014) Stable carbon isotope biogeochemistry of lakes along a trophic gradient. *Biogeosciences,* **11,** 6265-6276.

Deines, P., Bodelier, P.L. & Eller, G. (2007) Methane-derived carbon flows through methane-oxidizing bacteria to higher trophic levels in aquatic systems. *Environ Microbiol,* **9,** 1126-1134.

DelSontro, T., Beaulieu, J.J. & Downing, J.A. (2018) Greenhouse gas emissions from lakes and impoundments: Upscaling in the face of global change. *Limnology and Oceanography Letters,* **3,** 64-75.

DelVecchia, A.G., Stanford, J.A. & Xu, X. (2016) Ancient and methane-derived carbon subsidizes contemporary food webs. *Nature Communications,* **7,** 13163.

Dhellemmes, F., Smukall, M.J., Guttridge, T.L., Krause, J. & Hussey, N.E. (2021) Predator abundance drives the association between exploratory personality and foraging habitat risk in a wild marine meso-predator. *Functional Ecology,* **35,** 1972-1984.

Di Nezio, F., Beney, C., Roman, S., Danza, F., Buetti-Dinh, A., Tonolla, M. & Storelli, N. (2021) Anoxygenic photo- and chemo-synthesis of phototrophic sulfur bacteria from an alpine meromictic lake. *FEMS Microbiol Ecol,* **97**.

Docmac, F., Araya, M., Hinojosa, I.A., Dorador, C. & Harrod, C. (2017) Habitat coupling writ large: pelagic-derived materials fuel benthivorous macroalgal reef fishes in an upwelling zone. Wiley Online Library.

Donis, D., Flury, S., Stöckli, A., Spangenberg, J.E., Vachon, D. & McGinnis, D.F. (2017) Full-scale evaluation of methane production under oxic conditions in a mesotrophic lake. *Nature Communications,* **8,** 1661.

Downing, J.A., Prairie, Y.T., Cole, J.J., Duarte, C.M., Tranvik, L.J., Striegl, R.G., McDowell, W.H., Kortelainen, P., Caraco, N.F., Melack, J.M. & Middelburg, J.J. (2006) The

global abundance and size distribution of lakes, ponds, and impoundments. *Limnology and Oceanography,* **51,** 2388-2397.

Egerton, F.N. (2007) Understanding food chains and food webs, 1700–1970. *Bulletin of the Ecological Society of America,* **88,** 50-69.

Eglite, E., Mohm, C. & Dierking, J. (2023) Stable isotope analysis in food web research: Systematic review and a vision for the future for the Baltic Sea macro-region. *Ambio,* **52,** 319-338.

Finlay, J. & Kendall, C. (2007) Stable isotope tracing of organic matter sources and food web interactions in watersheds. pp. 283-333.

Fraterrigo, J.M. & Downing, J.A. (2008) The influence of land use on lake nutrients varies with watershed transport capacity. *Ecosystems,* **11,** 1021-1034.

Fry, B. (1991) Stable isotope diagrams of freshwater food webs. *Ecology,* **72,** 2293-2297.

Fry, B., Cox, J., Gest, H. & Hayes, J.M. (1986) Discrimination between 34S and 32S during bacterial metabolism of inorganic sulfur compounds. *Journal of Bacteriology,* **165,** 328-330.

Galloway, A.W., Brett, M.T., Holtgrieve, G.W., Ward, E.J., Ballantyne, A.P., Burns, C.W., Kainz, M.J., Müller-Navarra, D.C., Persson, J., Ravet, J.L., Strandberg, U., Taipale, S.J. & Alhgren, G. (2015) A Fatty Acid Based Bayesian Approach for Inferring Diet in Aquatic Consumers. *Plos One,* **10,** e0129723.

Gessner, M.O. & Chauvet, E. (1994) Importance of Stream Microfungi in Controlling Breakdown Rates of Leaf Litter. *Ecology,* **75,** 1807-1817.

Govan, E., Jackson, A.L., Bearhop, S., Inger, R., Stock, B.C., Semmens, B.X., Ward, E.J. & Parnell, A.C. (2024) cosimmr: an R package for fast fitting of Stable Isotope Mixing Models with covariates. *arXiv preprint arXiv:2408.17230*.

Grainger, R., Raoult, V., Peddemors, V.M., Machovsky-Capuska, G.E., Gaston, T.F. & Raubenheimer, D. (2023) Integrating isotopic and nutritional niches reveals multiple dimensions of individual diet specialisation in a marine apex predator. *Journal of Animal Ecology,* **92,** 514-534.

Greenhalgh, M. & Ovenden, D. (2007) *Freshwater life: Britain and northern Europe*. HarperCollins publishers.

Grossart, H.P., Van den Wyngaert, S., Kagami, M., Wurzbacher, C., Cunliffe, M. & Rojas-Jimenez, K. (2019) Fungi in aquatic ecosystems. *Nat Rev Microbiol,* **17,** 339-354.

Guggenheim, C., Freimann, R., Mayr, M.J., Beck, K., Wehrli, B. & Bürgmann, H. (2020) Environmental and Microbial Interactions Shape Methane-Oxidizing Bacterial Communities in a Stratified Lake. *Front Microbiol,* **11,** 579427.

Guillemette, F., von Wachenfeldt, E., Kothawala, D.N., Bastviken, D. & Tranvik, L.J. (2017) Preferential sequestration of terrestrial organic matter in boreal lake sediments. *Journal of Geophysical Research: Biogeosciences,* **122,** 863-874.

Harrod, C. & Grey, J. (2006) Isotopic variation complicates analysis of trophic relations within the fish community of Plußsee: a small, deep, stratifying lake. *Archiv fur Hydrobiologie,* **167,** 281-299.

Harrod, C. & Stallings, C. (2022) Trophodynamics. *Methods in fish biology, 2nd edn. American Fisheries Society, Bethesda*.

Havens, K. & Jeppesen, E. (2018) Ecological responses of lakes to climate change. pp. 917. MDPI.

Hayden, B., Harrod, C. & Kahilainen, K.K. (2014) Lake morphometry and resource polymorphism determine niche segregation between cool- and cold-water-adapted fish. *Ecology,* **95,** 538-552.

He, R., Wooller, M.J., Pohlman, J.W., Tiedje, J.M. & Leigh, M.B. (2015) Methane-derived carbon flow through microbial communities in arctic lake sediments. *Environ Microbiol,* **17,** 3233-3250.

Heikkinen, R., Hämäläinen, H., Kiljunen, M., Kärkkäinen, S., Schilder, J. & Jones, R.I. (2022) A Bayesian stable isotope mixing model for coping with multiple isotopes, multiple trophic steps and small sample sizes. *Methods in Ecology and Evolution,* **13,** 2586-2602.

Hessen, D.O., Andersen, T., Armstrong McKay, D., Kosten, S., Meerhoff, M., Pickard, A. & Spears, B.M. (2024) Lake ecosystem tipping points and climate feedbacks. *Earth Syst. Dynam.,* **15,** 653-669.

Hynes, H. (1950) The food of fresh-water sticklebacks (Gasterosteus aculeatus and Pygosteus pungitius), with a review of methods used in studies of the food of fishes. *The journal of animal ecology*, 36-58.

Itoh, M., Kojima, H., Ho, P.-C., Chang, C.-W., Chen, T.-Y., Hsiao, S.S.-Y., Kobayashi, Y., Fujibayashi, M., Kao, S.-J. & Hsieh, C.-h. (2017) Integrating isotopic, microbial, and modeling approaches to understand methane dynamics in a frequently disturbed deep reservoir in Taiwan. *Ecological research,* **32,** 861-871.

Jackson, A., Parnell, A. & Jackson, M.A. (2019) Package 'SIBER'. *R package version,* **2**.

James, R.H., Bousquet, P., Bussmann, I., Haeckel, M., Kipfer, R., Leifer, I., Niemann, H., Ostrovsky, I., Piskozub, J. & Rehder, G. (2016) Effects of climate change on methane emissions from seafloor sediments in the Arctic Ocean: A review. *Limnology and Oceanography,* **61,** S283-S299.

Jentzsch, K., Männistö, E., Marushchak, M.E., Korrensalo, A., van Delden, L., Tuittila, E.-S., Knoblauch, C. & Treat, C.C. (2024) Shoulder season controls on methane emissions from a boreal peatland. *Biogeosciences,* **21,** 3761-3788.

Jones, R.I. & Grey, J. (2011) Biogenic methane in freshwater food webs. *Freshwater Biology,* **56,** 213-229.

Kang, M., Liu, L. & Grossart, H.-P. (2024) Spatio-temporal variations of methane fluxes in sediments of a deep stratified temperate lake. *iScience,* **27**.

Kankaala, P., Taipale, S., Grey, J., Sonninen, E., Arvola, L. & Jones, R.I. (2006) Experimental d13C evidence for a contribution of methane to pelagic food webs in lakes. *Limnology and Oceanography,* **51,** 2821-2827.

Karlsson, J., Berggren, M., Ask, J., Byström, P., Jonsson, A., Laudon, H. & Jansson, M. (2012) Terrestrial organic matter support of lake food webs: Evidence from lake metabolism and stable hydrogen isotopes of consumers. *Limnology and Oceanography,* **57,** 1042-1048.

Karlsson, J., Byström, P., Ask, J., Ask, P., Persson, L. & Jansson, M. (2009) Light limitation of nutrient-poor lake ecosystems. *Nature,* **460,** 506-509.

Kiljunen, M., Grey, J., Sinisalo, T., Harrod, C., Immonen, H. & Jones, R.I. (2006) A revised model for lipid-normalizing δ13C values from aquatic organisms, with implications for isotope mixing models. *Journal of Applied Ecology,* **43,** 1213-1222.

Knowlton, M.F. & Jones, J.R. (2000) Non-Algal Seston, Light, Nutrients and Chlorophyll in Missouri Reservoirs. *Lake and Reservoir Management,* **16,** 322-332.

Kritzberg, E., Cole, J., Pace, M., Graneli, W. & Bade, D. (2004) Autochthonous versus allochthonous carbon sources to bacteria: Results from whole-lake 13C addition experiments. *Limnology and Oceanography,* **49**.

Kullberg, A., Hargeby, A., Petersen Jr, R., Bishop, K. & Jansson, M. (1993) The ecological significance of dissolved organic carbon in acidified waters. *Ambio (Journal of the Human Environment, Research and Management);(Sweden),* **22**.

Kurtul, I., Tarkan, A.S. & Britton, J.R. (2023) Inter-tissue variability in the stable isotope values of European perch (Perca fluviatilis) and pumpkinseed (Lepomis gibbosus). *Knowl. Manag. Aquat. Ecosyst.*, 22.

Laakso, T.A. & Schrag, D.P. (2019) Methane in the Precambrian atmosphere. *Earth and Planetary Science Letters,* **522,** 48-54.

Lammers, J.M., Reichart, G.J. & Middelburg, J.J. (2017) Seasonal variability in phytoplankton stable carbon isotope ratios and bacterial carbon sources in a shallow Dutch lake. *Limnology and Oceanography,* **62,** 2773-2787.

Lau, D.C., Sundh, I., Vrede, T., Pickova, J. & Goedkoop, W. (2014a) Autochthonous resources are the main driver of consumer production in dystrophic boreal lakes. *Ecology,* **95,** 1506-1519.

Lau, D.C.P., Sundh, I., Vrede, T., Pickova, J. & Goedkoop, W. (2014b) Autochthonous resources are the main driver of consumer production in dystrophic boreal lakes. *Ecology,* **95,** 1506-1519.

Le Cren, E.D. (1947) The Determination of the Age and Growth of the Perch (Perca fluviatilis) from the Opercular Bone. *Journal of Animal Ecology,* **16,** 188-204.

Lenz, J. (1977) Seston and Its Main Components. *Microbial Ecology of a Brackish Water Environment* (ed. G. Rheinheimer), pp. 37-60. Springer Berlin Heidelberg, Berlin, Heidelberg.

Liu, M., Raymond, P.A., Lauerwald, R., Zhang, Q., Trapp-Müller, G., Davis, K.L., Moosdorf, N., Xiao, C., Middelburg, J.J., Bouwman, A.F., Beusen, A.H.W., Peng, C., Lacroix, F., Tian, H., Wang, J., Li, M., Zhu, Q., Cohen, S., van Hoek, W.J., Li, Y., Li, Y., Yao, Y. & Regnier, P. (2024) Global riverine land-to-ocean carbon export constrained by observations and multi-model assessment. *Nature Geoscience,* **17,** 896-904.

Magen, C., Lapham, L.L., Pohlman, J.W., Marshall, K., Bosman, S., Casso, M. & Chanton, J.P. (2014) A simple headspace equilibration method for measuring dissolved methane. *Limnology and Oceanography: Methods,* **12,** 637-650.

Magnuson, J.J. (1990) Long-term ecological research and the invisible present. *BioScience,* **40,** 495-501.

Manko, P. (2016) Stomach content analysis in freshwater fish feeding ecology. *University of Prešov,* **116,** 1-25.

McCutchan, J.H., Lewis Jr, W.M., Kendall, C. & McGrath, C.C. (2003) Variation in trophic shift for stable isotope ratios of carbon, nitrogen, and sulfur. *Oikos,* **102,** 378-390.

McLachlan, A.J., Brennan, A. & Wotton, R.S. (1978) Particle size and chironomid (Diptera) food in an upland river. *Oikos*, 247-252.

Milferstedt, K., Youngblut, N.D. & Whitaker, R.J. (2010) Spatial structure and persistence of methanogen populations in humic bog lakes. *The ISME Journal,* **4,** 764-776.

Minick, K.J., Mitra, B., Noormets, A. & King, J.S. (2019) Saltwater reduces potential CO 2 and CH 4 production in peat soils from a coastal freshwater forested wetland. *Biogeosciences,* **16,** 4671-4686.

Moss, B. (1970) Seston Composition in Two Fresiiwater Pools. *Limnology and Oceanography,* **15,** 504-513.

Natchimuthu, S., Sundgren, I., Gålfalk, M., Klemedtsson, L., Crill, P., Danielsson, Å. & Bastviken, D. (2016) Spatio-temporal variability of lake CH4 fluxes and its influence on annual whole lake emission estimates. *Limnology and Oceanography,* **61,** S13-S26.

Newton, R.J., Kent, A.D., Triplett, E.W. & McMahon, K.D. (2006) Microbial community dynamics in a humic lake: differential persistence of common freshwater phylotypes. *Environmental Microbiology,* **8,** 956-970.

Ogle, D.H. (2018) *Introductory fisheries analyses with R*. Chapman and Hall/CRC.

Oksanen, J., Simpson, G.L., Blanchet, F.G., Kindt, R., Legendre, P., Minchin, P.R., O'hara, R., Solymos, P., Stevens, M.H.H. & Szoecs, E. (2001) Vegan: community ecology package. *(No Title)*.

Olson, C.R., Solomon, C.T. & Jones, S.E. (2020) Shifting limitation of primary production: experimental support for a new model in lake ecosystems. *Ecology letters,* **23,** 1800-1808.

Parnell, A. & Parnell, M.A. (2019) Package 'simmr'. *(2016) Aquaculture Big Numbers*. Food and Agriculture Organization of the United Nations Rome, Italy, Rome, Italy.

Pennington, W. & Tutin, T.G. (1974) Seston and Sediment Formation in Five Lake District Lakes. *Journal of Ecology,* **62,** 215-251.

Petta, J.C., Shipley, O.N., Wintner, S.P., Cliff, G., Dicken, M.L. & Hussey, N.E. (2020) Are you really what you eat? Stomach content analysis and stable isotope ratios do not uniformly estimate dietary niche characteristics in three marine predators. *Oecologia,* **192,** 1111-1126.

Phillips, D.L. (2012) Converting isotope values to diet composition: the use of mixing models. *Journal of Mammalogy,* **93,** 342-352.

Phillips, D.L. & Gregg, J.W. (2001) Uncertainty in source partitioning using stable isotopes. *Oecologia,* **127,** 171-179.

Phillips, D.L., Inger, R., Bearhop, S., Jackson, A.L., Moore, J.W., Parnell, A.C., Semmens, B.X. & Ward, E.J. (2014) Best practices for use of stable isotope mixing models in food-web studies. *Canadian Journal of Zoology,* **92,** 823-835.

Polito, M.J., Trivelpiece, W.Z., Karnovsky, N.J., Ng, E., Patterson, W.P. & Emslie, S.D. (2011) Integrating stomach content and stable isotope analyses to quantify the diets of pygoscelid penguins. *Plos One,* **6,** e26642.

Post, D.M. (2002) USING STABLE ISOTOPES TO ESTIMATE TROPHIC POSITION: MODELS, METHODS, AND ASSUMPTIONS. *Ecology,* **83,** 703-718.

Prchalová, M., Žák, J., Říha, M., Šmejkal, M., Blabolil, P., Vašek, M., Matěna, J., Peterka, J., Seďa, J. & Kubečka, J. (2022) Sexual size dimorphism of two common European percid fish: linkage with spatial distribution and diet. *Hydrobiologia,* **849,** 2009-2027.

Rantala, M.V., Meyer-Jacob, C., Kivilä, E.H., Luoto, T.P., Ojala, A.E.K., Smol, J.P. & Nevalainen, L. (2021) Traces of sunlight in the organic matter biogeochemistry of two shallow subarctic lakes. *Biogeochemistry,* **155,** 169-188.

Ravinet, M., Syväranta, J., Jones, R.I. & Grey, J. (2010) A trophic pathway from biogenic methane supports fish biomass in a temperate lake ecosystem. *Oikos,* **119,** 409-416.

Sabrekov, A.F., Semenov, M.V., Terentieva, I.E., Krasnov, G.S., Kharitonov, S.L., Glagolev, M.V. & Litti, Y.V. (2024) Anaerobic methane oxidation is quantitatively important in deeper peat layers of boreal peatlands: Evidence from anaerobic incubations, in situ stable isotopes depth profiles, and microbial communities. *Sci Total Environ,* **916,** 170213.

Sanseverino, A.M., Bastviken, D., Sundh, I., Pickova, J. & Enrich-Prast, A. (2012) Methane carbon supports aquatic food webs to the fish level.

Saunois, M., Stavert, A.R., Poulter, B., Bousquet, P., Canadell, J.G., Jackson, R.B., Raymond, P.A., Dlugokencky, E.J., Houweling, S. & Patra, P.K. (2019) The global methane budget 2000–2017. *Earth System Science Data Discussions,* **2019,** 1-136.

Savvichev, A.S., Kadnikov, V.V., Rusanov, I.I., Beletsky, A.V., Krasnova, E.D., Voronov, D.A., Kallistova, A.Y., Veslopolova, E.F., Zakharova, E.E., Kokryatskaya, N.M., Losyuk, G.N., Demidenko, N.A., Belyaev, N.A., Sigalevich, P.A., Mardanov, A.V., Ravin, N.V. &

Pimenov, N.V. (2020) Microbial Processes and Microbial Communities in the Water Column of the Polar Meromictic Lake Bol'shie Khruslomeny at the White Sea Coast. *Frontiers in Microbiology,* Volume 11 - 2020.

Sayle, K., Cook, G., Ascough, P., Kinch, H., McGovern, T., Hicks, M., Fridriksson, A., Einarsson, Á. & Edwald Maxwell, Á. (2013) Application of 34 S analysis for elucidating terrestrial, marine and freshwater ecosystems: Evidence of animal movement/husbandry practices in an early Viking community around Lake Myvatn, Iceland. *Geochimica et Cosmochimica Acta,* **120,** 531-544.

Schenk, J., Sawakuchi, H.O., Sieczko, A.K., Pajala, G., Rudberg, D., Hagberg, E., Fors, K., Laudon, H., Karlsson, J. & Bastviken, D. (2021) Methane in Lakes: Variability in Stable Carbon Isotopic Composition and the Potential Importance of Groundwater Input. *Frontiers in Earth Science,* Volume 9 - 2021.

Schorn, S., Graf, J.S., Littmann, S., Hach, P.F., Lavik, G., Speth, D.R., Schubert, C.J., Kuypers, M.M.M. & Milucka, J. (2024) Persistent activity of aerobic methane-oxidizing bacteria in anoxic lake waters due to metabolic versatility. *Nat Commun,* **15,** 5293.

Seekell, D., Lapierre, J.-F., Ask, J., Bergström, A.-K., Deininger, A., Rodriguez, P. & Karlsson, J. (2015) The influence of dissolved organic carbon on primary production in northern lakes: Influence of DOC on production. *Limnology and Oceanography,* **60**.

Shafi, M. (1969) *Comparative studies of populations of perch (Perca fluviatilis L.) and pike (Esox lucius L.) in two Scottish lochs*. University of Glasgow (United Kingdom).

Shafi, M. & Maitland, P.S. (1971) The age and growth of perch (Perca fluviatilis L.) in two Scottish lochs. *Journal of Fish Biology,* **3,** 39-57.

Stenzel, B., Rofner, C., Pérez, M.T. & Sommaruga, R. (2017) Stoichiometry of natural bacterial assemblages from lakes located across an elevational gradient. *Scientific Reports,* **7,** 5875.

Syväranta, J., Lensu, A., Marjomäki, T.J., Oksanen, S. & Jones, R.I. (2013) An Empirical Evaluation of the Utility of Convex Hull and Standard Ellipse Areas for Assessing Population Niche Widths from Stable Isotope Data. *Plos One,* **8,** e56094.

Tadonléké, R.D., Planas, D. & Lucotte, M. (2005) Microbial food webs in boreal humic lakes and reservoirs: ciliates as a major factor related to the dynamics of the most active bacteria. *Microb Ecol,* **49,** 325-341.

Tanentzap, A.J., Kielstra, B.W., Wilkinson, G.M., Berggren, M., Craig, N., del Giorgio, P.A., Grey, J., Gunn, J.M., Jones, S.E., Karlsson, J., Solomon, C.T. & Pace, M.L. (2017) Terrestrial support of lake food webs: Synthesis reveals controls over cross-ecosystem resource use. *Science Advances,* **3,** e1601765.

Tarkan, A.S., Haubrock, P.J., Aksu, S., Mol, O., Balzani, P., Emiroğlu, Ö., Köse, E., Kurtul, I., Başkurt, S., Çınar, E. & Oztopcu-Vatan, P. (2023) Predicting the potential implications of perch (Perca fluviatilis) introductions to a biodiversity-rich lake using stable isotope analysis. *Scientific Reports,* **13,** 17635.

Tarkowska-Kukuryk, M. (2013) Periphytic algae as food source for grazing chironomids in a shallow phytoplankton-dominated lake. *Limnologica,* **43,** 254-264.

Thomas, S.M. & Crowther, T.W. (2015) Predicting rates of isotopic turnover across the animal kingdom: a synthesis of existing data. *Journal of Animal Ecology,* **84,** 861-870.

Tippett, R. (1994) The ecology of pelagic communities in Lochan Dubh. *The Ecology of Loch Lomond* (eds K.J. Murphy, M.C.M. Beveridge & R. Tippett), pp. 153-166. Springer Netherlands, Dordrecht.

Tokeshi, M. (1986) Resource utilization, overlap and temporal community dynamics: a null model analysis of an epiphytic chironomid community. *The journal of animal ecology*, 491-506.

Tranvik, L.J., Cole, J.J. & Prairie, Y.T. (2018) The study of carbon in inland waters—from isolated ecosystems to players in the global carbon cycle. *Limnology and Oceanography Letters,* **3,** 41-48.

Tranvik, L.J., Downing, J.A., Cotner, J.B., Loiselle, S.A., Striegl, R.G., Ballatore, T.J., Dillon, P., Finlay, K., Fortino, K. & Knoll, L.B. (2009) Lakes and reservoirs as regulators of carbon cycling and climate. *Limnology and Oceanography,* **54,** 2298-2314.

Tsuchiya, K., Komatsu, K., Shinohara, R., Imai, A., Matsuzaki, S.-i.S., Ueno, R., Kuwahara, V.S. & Kohzu, A. (2020) Variability of benthic methane-derived carbon along seasonal, biological, and sedimentary gradients in a polymictic lake. *Limnology and Oceanography,* **65,** 3017-3031.

van Grinsven, S., Sinninghe Damsté, J.S., Abdala Asbun, A., Engelmann, J.C., Harrison, J. & Villanueva, L. (2020) Methane oxidation in anoxic lake water stimulated by nitrate and sulfate addition. *Environ Microbiol,* **22,** 766-782.

Vejříková, I., Vejřík, L., Čech, M., Blabolil, P. & Peterka, J. (2023) Variable diet plasticity in Eurasian perch (Perca fluviatilis): Current versus seasonal food uptake. *Ecology of Freshwater Fish,* **32,** 795-803.

Wada, E. (2009) Stable delta(15)N and delta(13)C isotope ratios in aquatic ecosystems. *Proc Jpn Acad Ser B Phys Biol Sci,* **85,** 98-107.

Wagner, A., Volkmann, S. & Dettinger-Klemm, P.M.A. (2012) Benthic–pelagic coupling in lake ecosystems: the key role of chironomid pupae as prey of pelagic fish. *Ecosphere,* **3,** art14.

Woolway, R.I., Sharma, S., Weyhenmeyer, G.A., Debolskiy, A., Golub, M., Mercado-Bettín, D., Perroud, M., Stepanenko, V., Tan, Z. & Grant, L. (2021) Phenological shifts in lake stratification under climate change. *Nature Communications,* **12,** 2318.

Xi, X., Zhuang, Q., Kim, S. & Zhang, Z. (2023) Methane emissions from land and aquatic ecosystems in western Siberia: An analysis with methane biogeochemistry models. *Journal of Geophysical Research: Biogeosciences,* **128,** e2023JG007466.

Yang, J., Zhang, P., Cai, M., Han, M., Wu, Z., Xiao, H., Han, J., Zhang, X., Dong, H. & Jiang, H. (2025) Methanogenesis rather than carbon dioxide production drives positive priming effects in anoxic sediments of saline lakes. *Chemical Geology,* **678,** 122680.

Yang, S., Anthony, S.E., Jenrich, M., in't Zandt, M.H., Strauss, J., Overduin, P.P., Grosse, G., Angelopoulos, M., Biskaborn, B.K. & Grigoriev, M.N. (2023) Microbial methane cycling in sediments of Arctic thermokarst lagoons. *Global Change Biology,* **29,** 2714-2731.

Yeakel, J.D., Bhat, U., Elliott Smith, E.A. & Newsome, S.D. (2016a) Exploring the Isotopic Niche: Isotopic Variance, Physiological Incorporation, and the Temporal Dynamics of Foraging. *Frontiers in Ecology and Evolution,* **Volume 4 - 2016**.

Yeakel, J.D., Bhat, U., Elliott Smith, E.A. & Newsome, S.D. (2016b) Exploring the isotopic niche: Isotopic variance, physiological incorporation, and the temporal dynamics of foraging. *Frontiers in Ecology and Evolution,* **4,** 1.

Youngblut, N.D., Dell'aringa, M. & Whitaker, R.J. (2014) Differentiation between sediment and hypolimnion methanogen communities in humic lakes. *Environ Microbiol,* **16,** 1411-1423.

Yun, H.Y., Kim, S., Choi, H., Kim, J.-E., Park, S.R. & Shin, K.-H. (2024) Essential amino acid carbon isotope ratios as indicators of marine macrophyte response to environmental variation. *Frontiers in Marine Science,* Volume 11 - 2024.

Zigah, P.K. (2013) Sources, biogeochemical cycling, and fate of organic matter in Lake Superior: An investigation using natural abundance radiocarbon and stable isotopes. University of Minnesota.

Appendix

A1. Table for $\delta^{13}C$ and $\delta^{15}N$ analysis values for all processed samples.

Appendix A1*. Bulk stable isotope values ($\delta^{13}C$, $\delta^{15}N$), elemental composition (%C, %N), and C:N ratios (mean ± SD) of fish, invertebrates, zooplankton, photosynthetic sources, bacteria, and organic matter collected from the study system. Putative trophic positions (T. P) are assigned based on taxonomic identity and ecological role. Sample sizes (n) are given for each taxon.*

Functional group	Species (n = sample size)	Putative T.P.	Mean ± S.D.				
			$\delta^{13}C$	$\delta^{15}N$	%C	%N	C:N
Fish	Perch (n = 127)	3.5-4	-25.8 ± 1.2	7.8 ± 0.8	47.9± 2.6	14.1 ± 0.8	3.4 ± 0.2
	Pike (n = 10)	4-4.5	-24.8 ± 1.0	9.1 ± 1.2	44.2 ± 5.8	13.7 ± 1.8	3.2 ± 0.1
Invertebrates	Asellus (n = 6)	2	-36.9 ± 0.6	0.8 ± 0.6	36.7 ± 3.9	8.4 ± 0.7	4.4 ± 0.4
	Chironomidae (n = 11)	2	-35.3 ± 0.7	2.8 ± 0.7	47.5 ± 3.2	10.5 ± 1.6	4.6 ± 0.6
	Chrysomelidae (n = 2)	2	-26.6 ± 2.7	4.9± 1.0	49.2 ± 2.2	11.2 ± 0.5	4.5 ± 0.2
	Chaoboridae (n = 10)	3	-29.9 ± 1.4	5.9 ± 0.7	45.0 ± 6.6	8.9 ± 2.3	5.2 ± 1.2
	Corixidae (n = 3)	2	-31.0 ± 2.8	3.0 ± 0.3	48.7 ± 1.6	10.9 ± 0.5	4.5 ± 0.1

	Ephemeroptera n (n = 1)	3	-32.6 ± 0.1	3.8 ± 0.1	51.3 ± 0.1	12.4 ± 0.1	4.1 ± 0.1
	Gammaridae (n = 2)	2	-32.6 ± 2.0	3.2 ± 0.6	43.3 ± 3.4	9.0 ± 0.1	4.8 ± 0.3
	Gomphidae (n = 2)	3	-31.4 ± 0.5	3.0± 0.1	45.3 ± 0.5	3.0 ± 0.1	4.3± 0.5
	Gyrinidae (n = 3)	3	-30.1 ± 0.4	2.9 ± 0.3	46.9 ± 0.2	10.0 ± 0.5	4.7± 0.2
	Hydracarina (n =3)	3	-31.4 ± 1.3	5.6 ± 0.7	54.4 ± 1.5	9.7 ± 0.4	5.6 ± 0.3
	Piscicolidae (n = 1)	3	-30.0 ± 0.1	6.5 ± 0.1	57.4 ± 0.1	9.7 ± 0.1	5.9 ± 0.1
	Notonectidae (n = 7)	3	-31.0 ± 1.4	3.7 ± 0.9	49.6 ± 1.5	11.9 ± 0.6	4.2 ± 0.2
	Sialidae (n = 3)	3	-31.9 ± 1.4	3.0 ± 0.2	49.7 ± 1.1	11.0 ± 0.6	4.5 ± 0.3
	Tetragnathidae (n = 3)	3.5-4	-30.6 ± 0.2	8.4 ± 0.2	49.9 ± 1.9	10.9 ± 0.7	4.6 ± 0.1
	Trichoptera (n = 2)	3	-32.6 ± 0.6	2.1 ± 1.2	56.6 ± 1.3	9.0 ± 1.3	6.4 ± 0.8
	Gerridae (n = 1)	3	-30.5 ± 0.1	7.7 ± 0.1	50.7 ± 0.1	10.8 ± 0.1	4.8 ± 0.1
	Pentatomidae (n = 3)	3	-27.7 ± 0.4	1.3± 1.3	47.9 ± 4.8	11.0 ± 1.0	4.4 ± 0.2
Zooplankton	**Eudiaptomus (n = 4)**	3	-32.5 ± 0.3	6.8 ± 2.3	39.8 ± 3.0	8.2 ± 0.9	4.9 ± 0.3
	Mesocyclops (n = 3)	3	-31.5 ± 3.4	3.6 ± 1.8	47.4 ± 4.2	9.7 ± 0.2	4.9 ±0.5
	Ceriodaphnia (n = 1)	2	-28.3 ± 0.1	-2.3 ± 0.1	38.4 ± 0.1	2.8 ± 0.1	13.7± 0.1
	Holopedium (n = 1)	2	-29.9 ± 0.1	5.1 ± 0.1	40.7 ± 0.1	8.8 ± 0.1	4.6 ± 0.1

Photosynthetic sources	**Biofilm (n = 3)**	1	-29.4 ± 0.5	0.5 ± 0.9	43.7 ± 1.2	1.1 ± 0.2	42.4 ± 6.9
	Nuphar (n = 3)	1	-26.0 ± 0.1	0.4 ± 0.2	44.5 ± 0.4	2.4 ± 0.1	18.3 ± 0.3
	Nymphea (n = 3)	1	-26.4 ± 0.2	2.1 ± 0.6	46.25 ± 0.22	1.96 ± 0.01	23.57 ± 0.12
	Potamogeton (n = 3)	1	-29.0 ± 0.5	0.8 ± 0.5	44.6 ± 0.1	1.0 ± 0.1	46.1 ± 1.4
	Phragmites (n = 10)	1	-29.6 ± 0.5	0.4 ± 1.1	43.9 ± 1.4	1.0 ± 0.2	50.2 ± 4.0
	Leaf litter (n = 5)	1	-32.4 ± 0.2	-1.9 ± 0.9	41.6 ± 1.1	1.2 ± 0.1	27.4 ± 2.4
	Terrestrial leaf litter (n = 5)	1	-31.1 ± 0.7	-4.4 ± 0.5	50.4 ± 0.7	1.2 ± 0.3	43.2 ± 8.0
Bacteria	**Methane-oxidising bacteria (MOB) (n = 15) from Lau *et al.* (2014b)**	1	-60.00 ± 1.0	-2.8 ± 1.0	48.0 ± 2.0	8.0 ± 0.5	6.0 ± 0.1
Organic matter	**Seston (n = 3)**	1	-30.64 ± 0.27	-0.80 ± 0.65	24.29 ± 4.37	1.68 ± 0.12	14.62 ± 3.75
	Particulate organic matter (POM) (n = 5)	1	-28.4 ± 0.2	2.3 ± 1.2	45.0± 0.5	1.2 ± 0.1	37.5 ± 0.1

A2. Length at 50% maturity

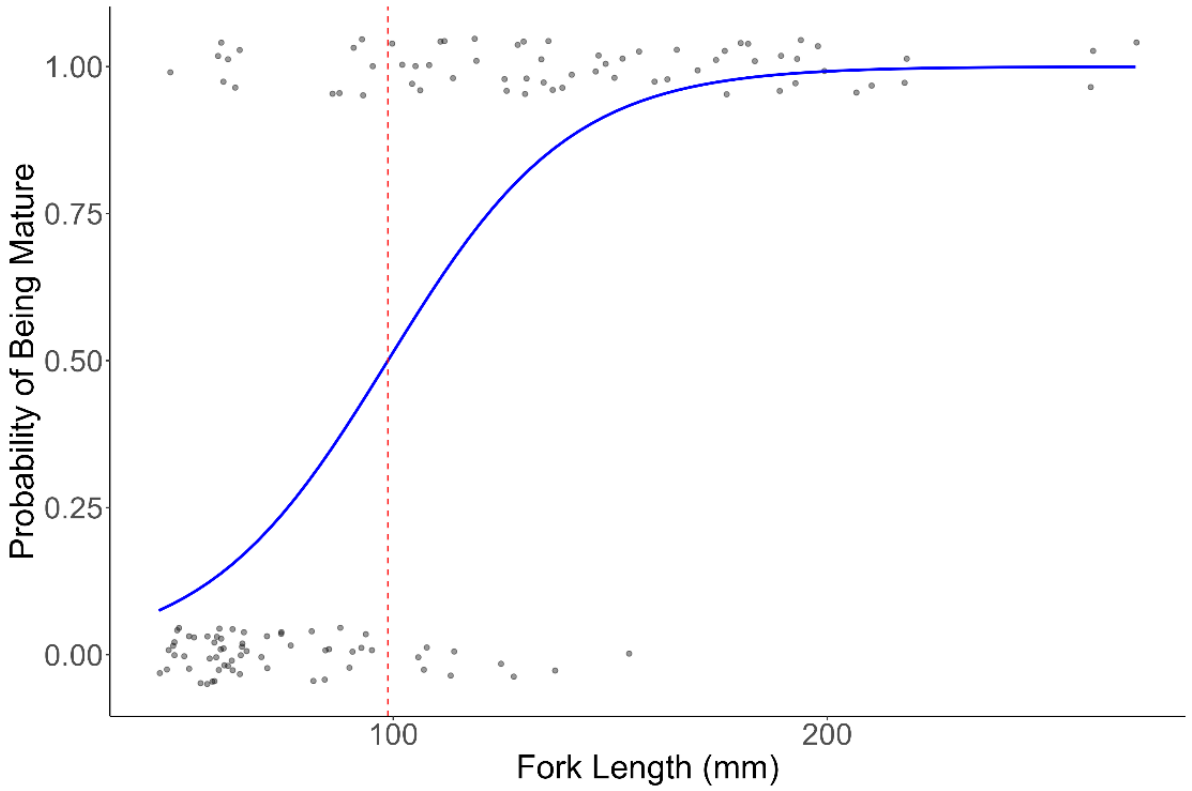

Appendix A2. *Length at 50% maturity (L_{50} = 99 mm) for perch (Perca fluviatilis), estimated from maturity ogive analysis. The proportion of mature individuals increases with body length.*

A3. Fork length (FL) and mass by Sex

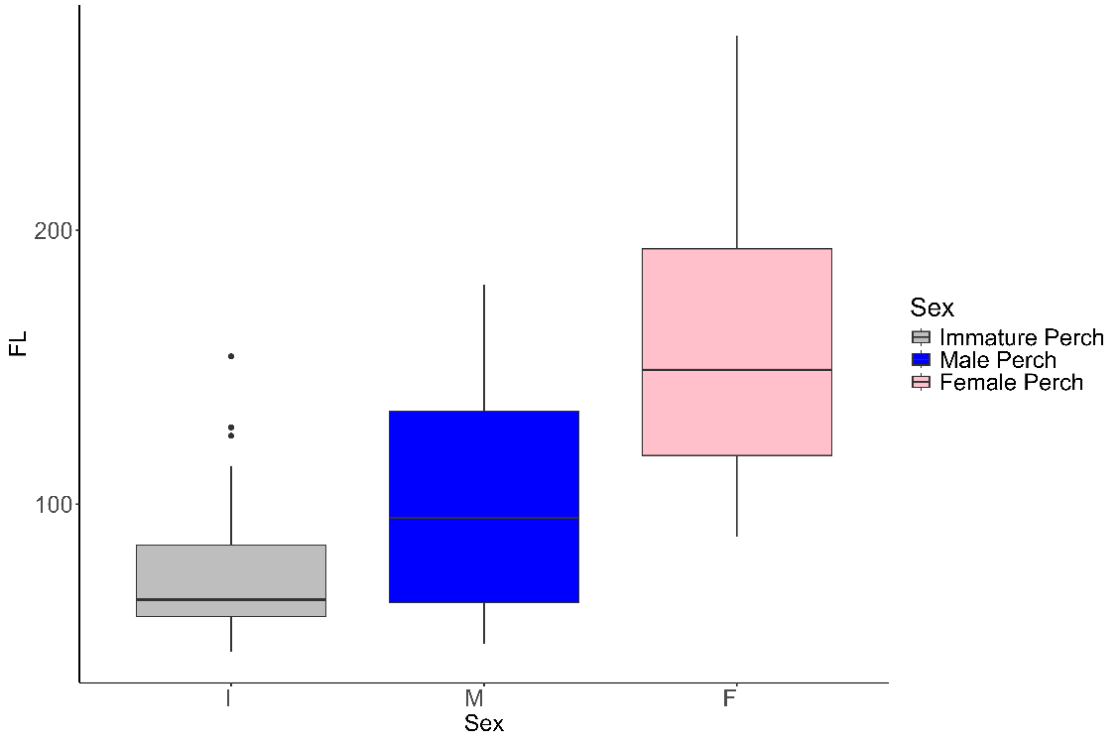

Appendix 3(1). *Boxplot of perch (Perca fluviatilis) fork length (FL) by sex, showing that females attain significantly larger body sizes than males. Boxes represent interquartile ranges, horizontal lines indicate medians, and whiskers denote variability outside the upper and lower quartiles.*

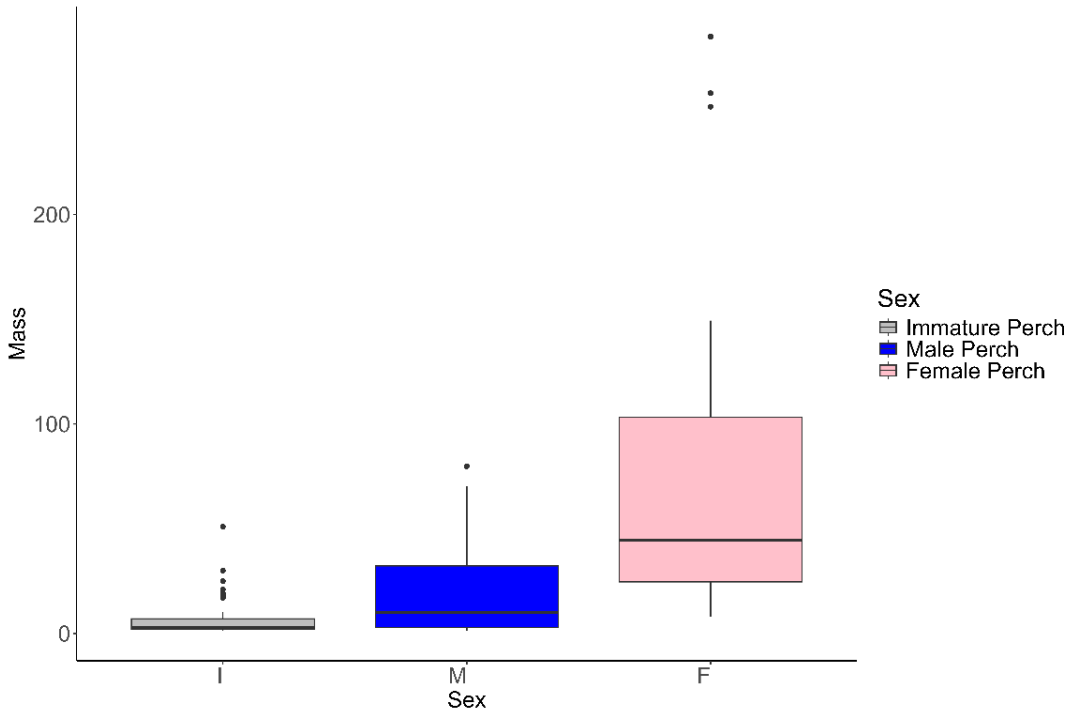

Appendix 3(2). *Boxplot of perch (Perca fluviatilis) body mass by sex, indicating that females are generally heavier than males. Boxes show interquartile ranges, horizontal lines represent medians, and whiskers denote variability outside the quartiles.*

A4. Age structure in European perch

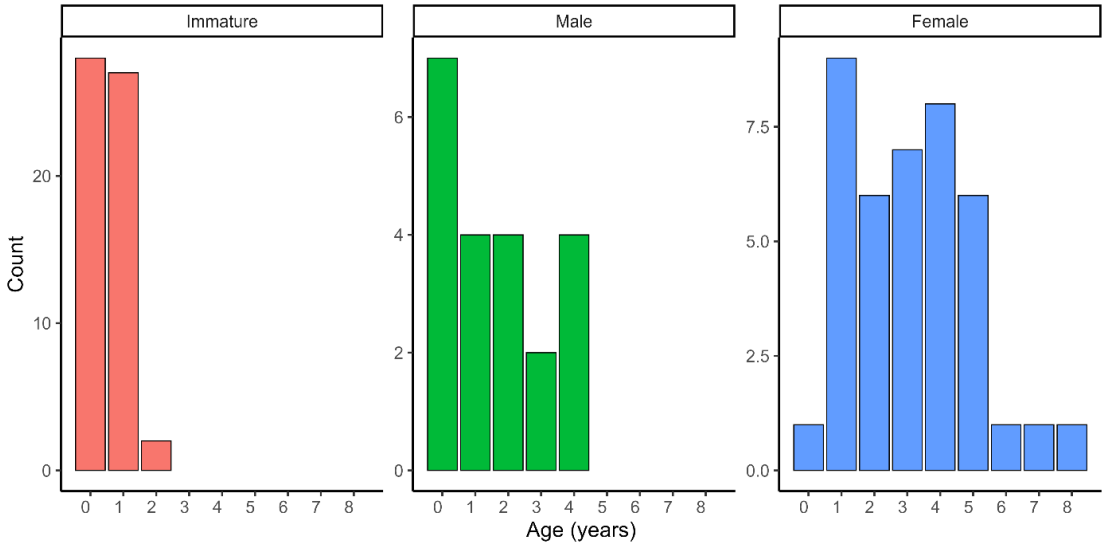

Appendix A4. *Age distribution of perch (Perca fluviatilis) by sex. Female perch tended to be older than males, as indicated by the counts across age classes. Data are shown separately for each sex.*

A5. Size at age by sex in European perch

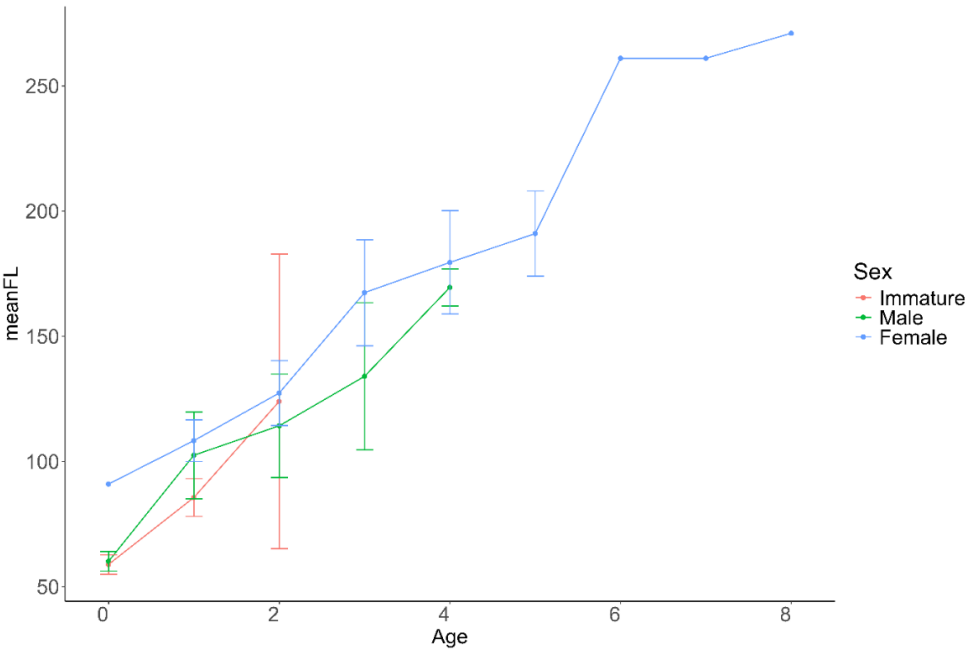

Appendix A5. *Growth of perch (Perca fluviatilis) across age classes, shown separately for immatures, males and females. Females generally attain larger lengths than males at each age, illustrating sexual dimorphism in growth patterns*

A6. Dissolved oxygen contour plot

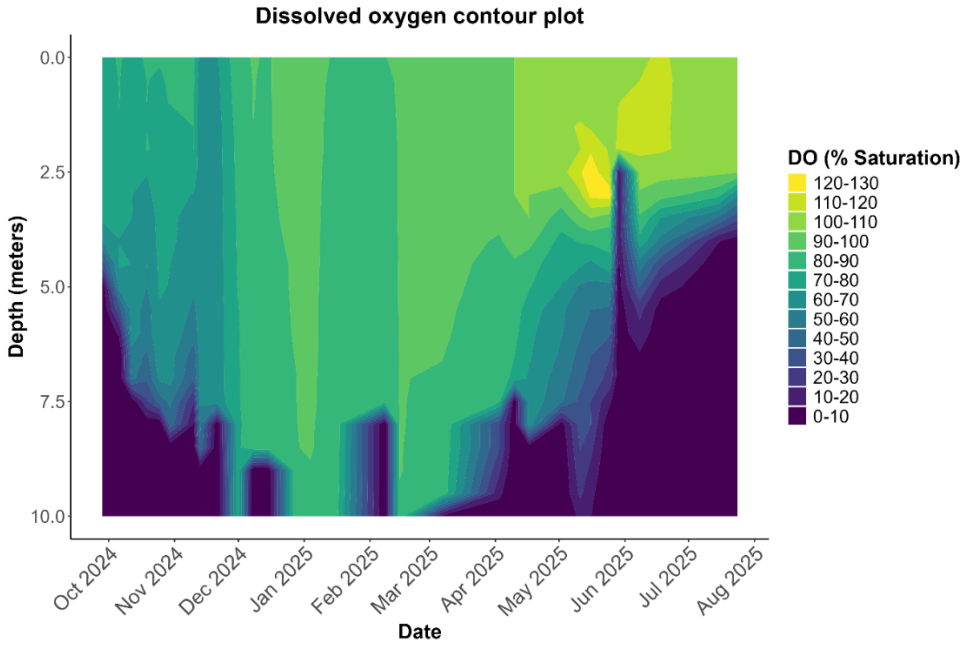

Appendix A6. *Dissolved oxygen profiles in Dubh Lochan from October 2024 to August 2025. The contour plot illustrates seasonal oxygen stratification, highlighting periods and depths of hypoxia and anoxia within the water column.*

A7. Temperature contour plot

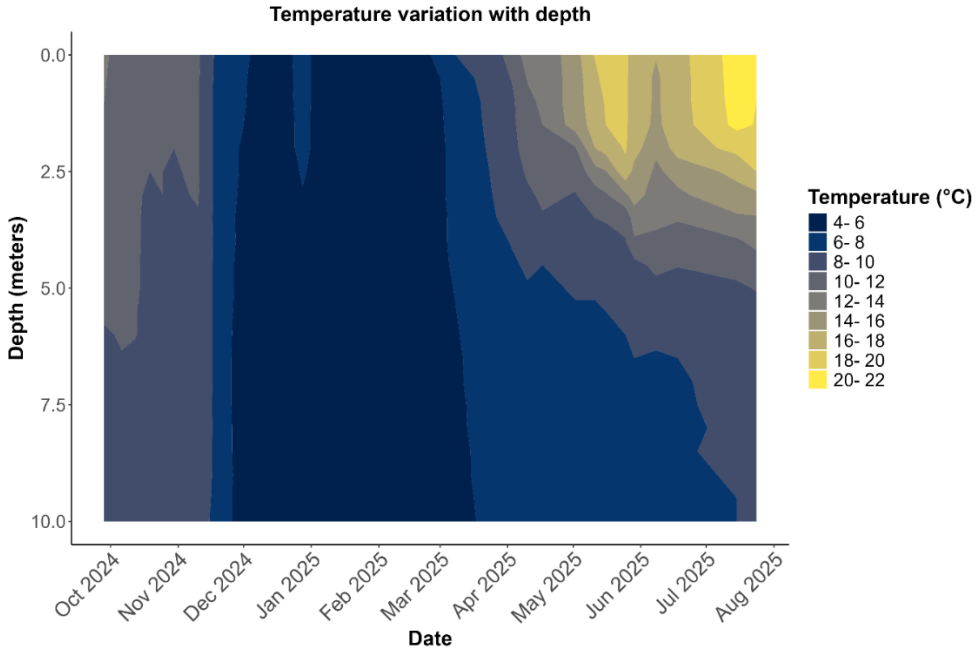

Appendix A7. *Temperature profiles of Dubh Lochan from October 2024 to August 2025. The plot shows seasonal thermal stratification during summer and complete mixing in winter, consistent with monomictic lake dynamics.*

A8. Light contour plot

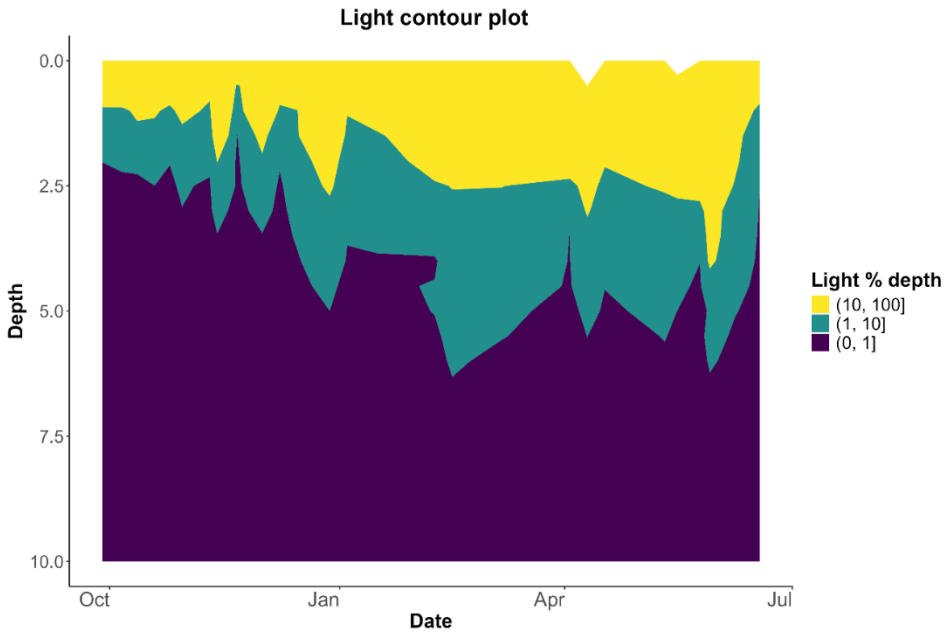

Appendix A8. *Light attenuation in Dubh Lochan from October 2024 to August 2025. The Secchi depth measured 2.25 m, indicating that the euphotic zone extends roughly 2–6 m depending on seasonal variation.*

A9. Ordered boxplot for d13C

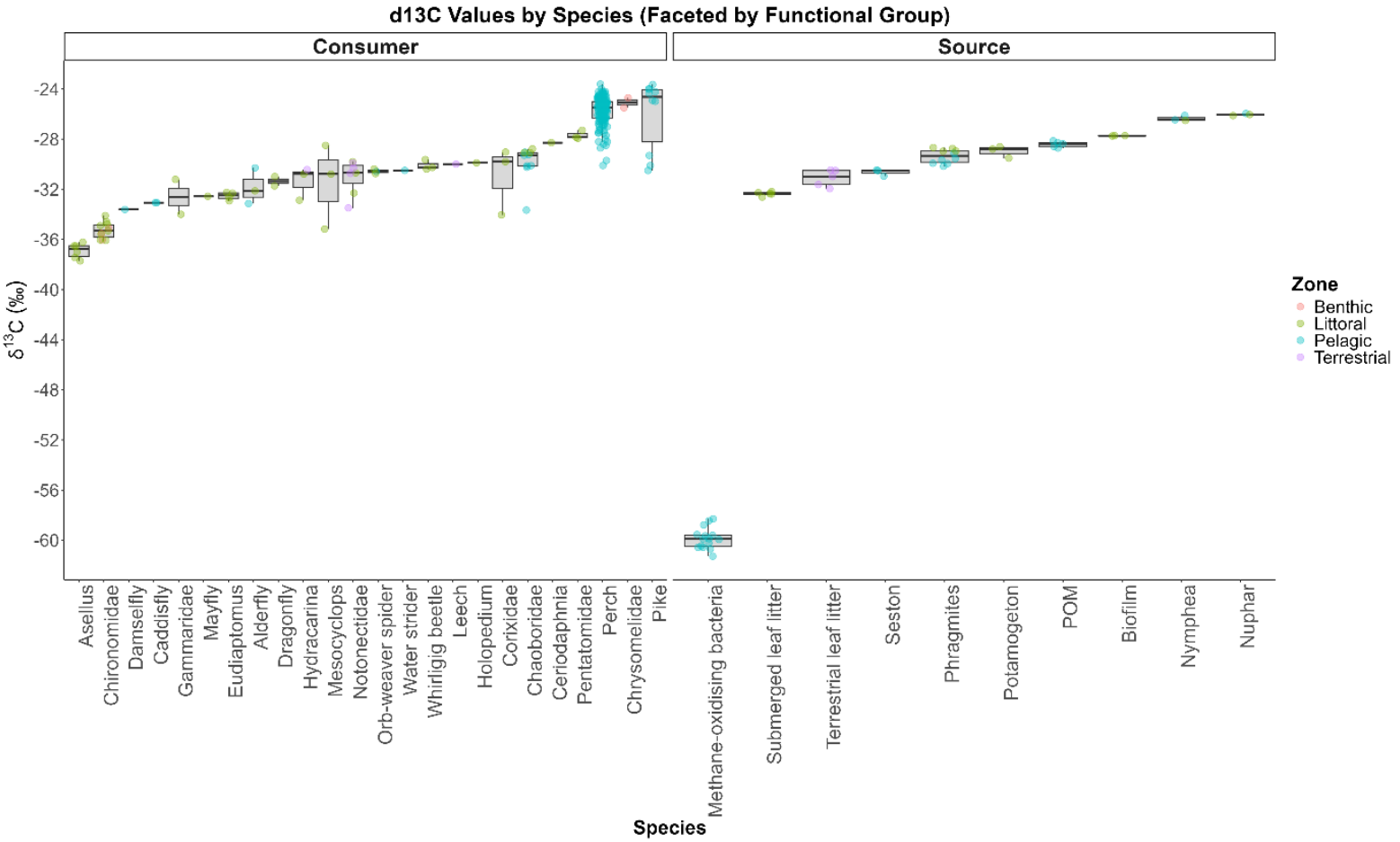

Appendix A9. *Boxplot of δ¹³C values for different taxa, ordered by increasing δ¹³C. Taxa are grouped into sources and consumers to illustrate differences in carbon signatures across the food web.*

A10. Ordered boxplot of d15N

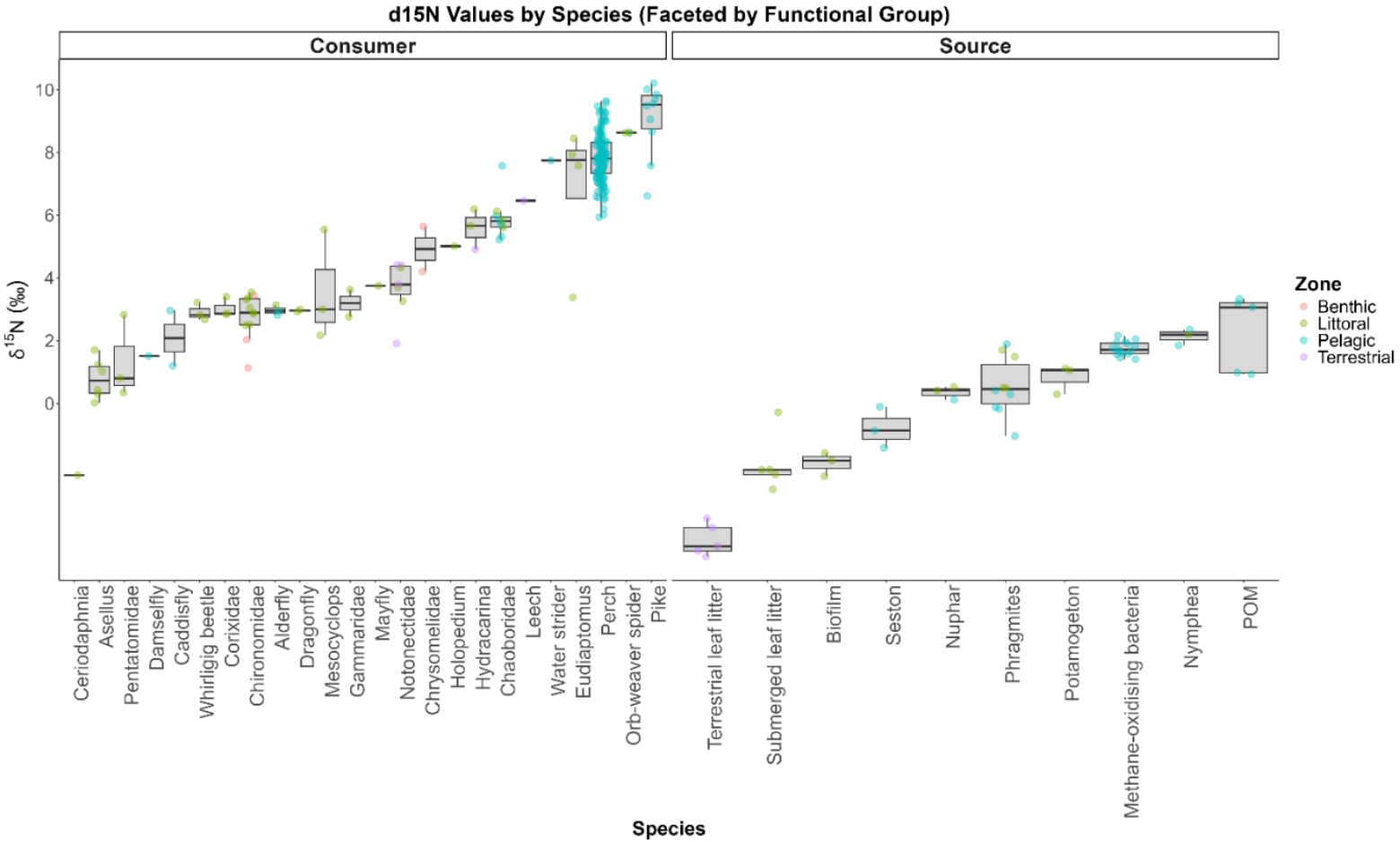

Appendix A10. *Boxplot of $\delta^{13}C$ values for different taxa, ordered by increasing $\delta^{13}C$. Taxa are grouped into sources and consumers to illustrate differences in carbon signatures across the food web.*

A11: LOESS for $\delta^{13}C$ against fork length

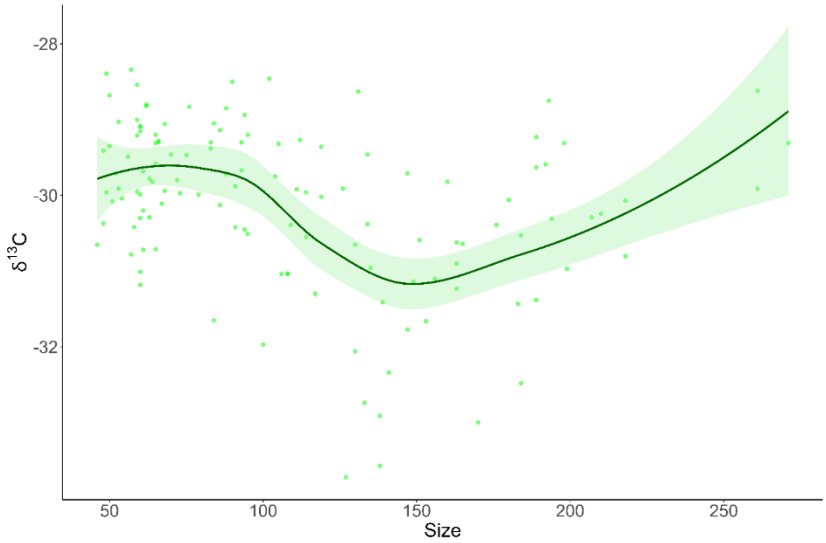

Appendix A11. *Loess-smoothed relationship between $\delta^{13}C$ values and individual size, illustrating how carbon isotopic signatures vary with growth across sampled taxa.*

A12: LOESS for $\delta^{15}N$ against fork length

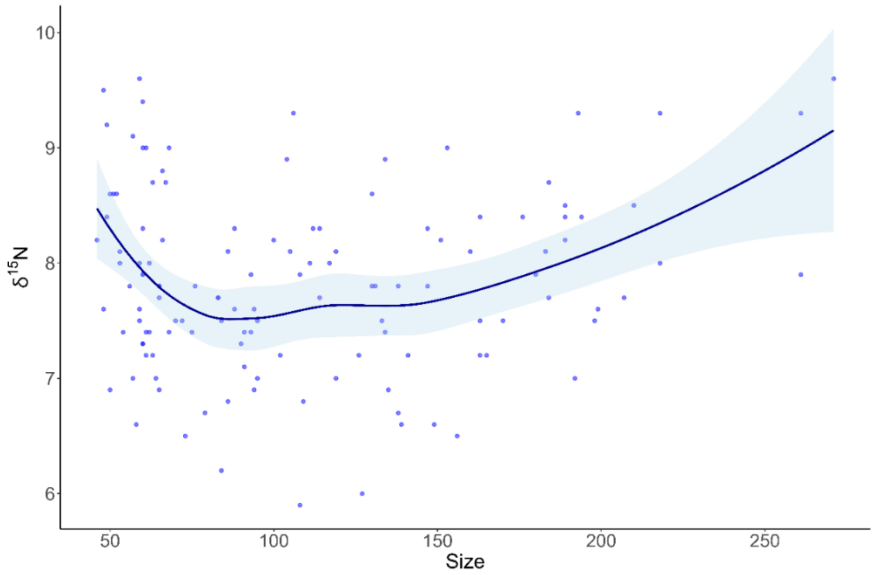

Appendix A12. *Loess-smoothed relationship between $\delta^{15}N$ values and individual size, showing how nitrogen isotopic signatures change with growth and potentially indicate shifts in trophic position.*

A13: SIBER ellipses on size classes of perch

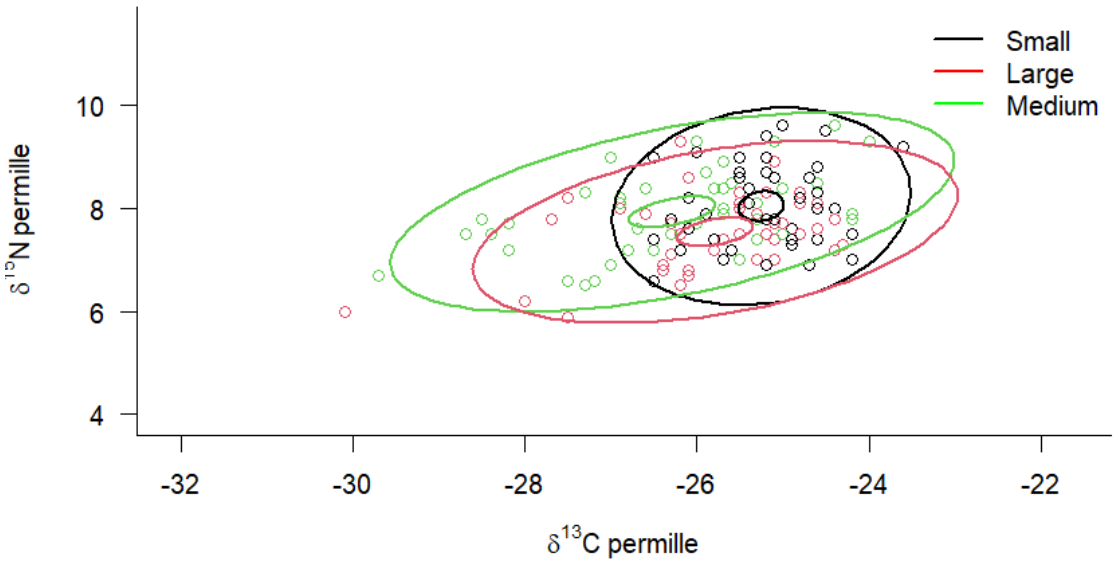

Appendix A13. *SIBER-derived convex hull ellipses illustrating the isotopic niche width of small, medium, and large perch, highlighting changes in niche size and trophic variability across size classes.*

A14: SIBER comparison by size class of perch

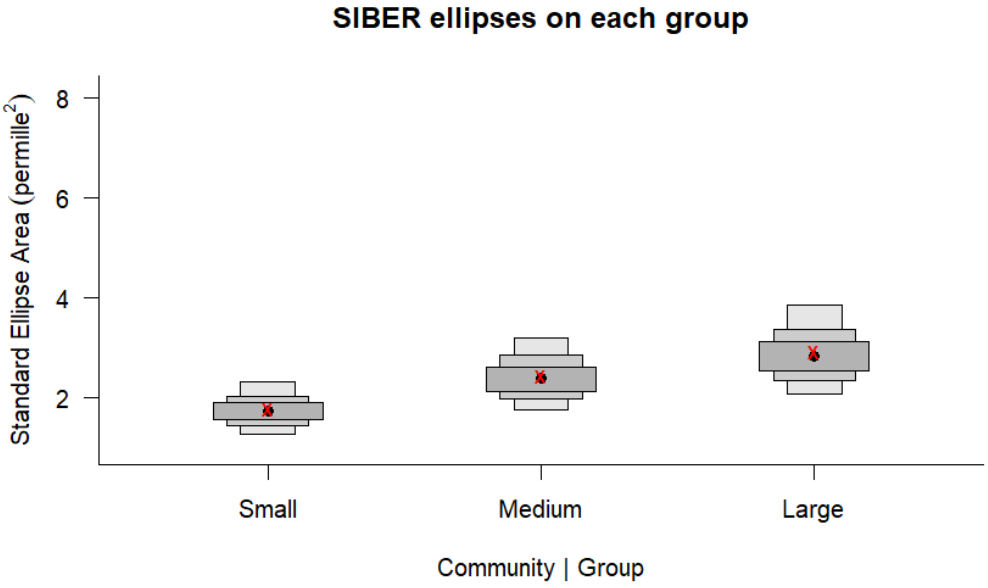

Appendix A14. *Comparison of standard ellipse areas (SEAs) for perch size classes relative to the overall community using SIBER, showing how isotopic niche width varies among small, medium, and large perch.*

Academic Integrity/ AI Declaration

Course Code: BIOL5187P

Course Title: MRes Ecology and Environmental Biology

Assessment: Final Report

If you have or haven't used generative AI tools, you must complete the declaration. You can write in bullet points or in a paragraph. We will use this information to ensure that we give appropriate and useful feedback.

Appropriate use of AI tools (see the Academic Integrity/AI statement for this assessment) will not detrimentally affect your grade but undeclared or inappropriate use is subject to academic misconduct procedures.

I have~~/have not~~ used AI tools to support this assignment.

What AI tools did you use and what tasks did you use them for?

- *ChatGPT, as a tool for explaining new concepts*

Which section(s) contain the results of AI tools and how did you incorporate AI use in your text and/or script?

- *NA*
- *Me: Hey GPT, what is thermal stratification?*

  ChatGPT: Thermal stratification is the ***layering of water in lakes, reservoirs, or other standing water bodies due to differences in temperature and density****. Because water density changes with temperature, lakes often separate into distinct layers during warmer months:*

1. ***Epilimnion*** *– The upper, warm, and well-mixed layer. It receives sunlight, so it's usually rich in oxygen and supports most aquatic life.*
2. ***Metalimnion (Thermocline)*** *– The middle layer where temperature changes rapidly with depth. It acts as a barrier to mixing between surface and deeper waters.*
3. ***Hypolimnion*** *– The bottom, colder, and denser layer. It's isolated from surface mixing, so oxygen can become depleted over time.*

*This stratification usually develops in **summer** (in temperate regions) and breaks down in **autumn and spring** when surface cooling and wind mixing cause the water column to turn over (mix completely). In **winter**, lakes in colder climates may also stratify beneath ice, with slightly warmer (4 °C) water at the bottom and near-freezing water at the top.*

*Stratification is crucial in **lake ecology** because it controls oxygen availability, nutrient cycling, and the distribution of organisms.*

☑ I confirm that the report submitted is exclusively my own work, with any external assistance explicitly acknowledged in the box above.

GUID: 3008817W Date: 19 August 2025